

©Prof. Roger G. Mark, 2004

MASSACHUSETTS INSTITUTE OF TECHNOLOGY

**Departments of Electrical Engineering, Mechanical Engineering,
and the Harvard-MIT Division of Health Sciences and Technology**

6.022J/2.792J/HST542J: Quantitative Physiology: Organ Transport Systems

CARDIOVASCULAR MECHANICS I, II, III

- I. Models of the Peripheral Circulation
- II. The Heart as a Pump
- III. Modeling of the Intact System

Text References:

- I. pages 101-115
- II. pages 126-139
- III. pages 139-144

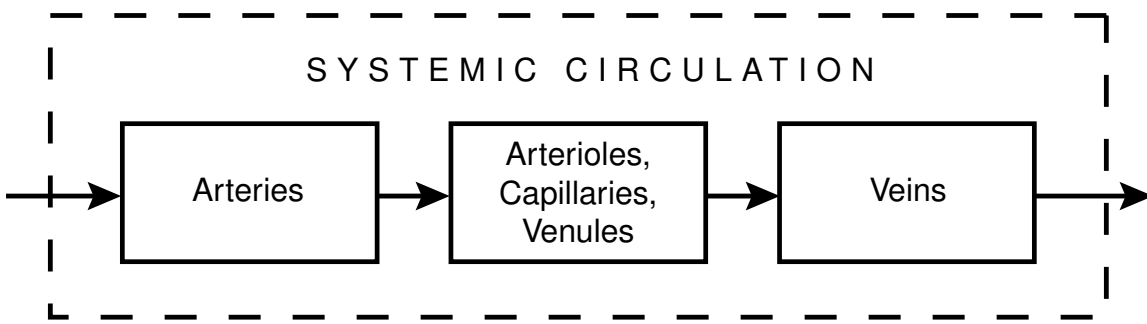
I. MODELS OF THE PERIPHERAL CIRCULATION

A. Introduction

Our objective in this section is to develop a simple conceptual and analytical model for the vasculature which will be valid for both steady and pulsatile flows. We will, however, limit ourselves to lumped parameter models, and will not discuss distributed-parameter transmission line type models. Hence, we will be able to discuss both average and pulsatile flows, volumes and pressures, at selected points in the vascular bed, but we cannot discuss pulse wave propagation, reflections, detailed fluid flow behavior, etc.

There are three major functional components in the systemic vascular bed: the elastic arteries, the microcirculation (including arterioles, capillaries, and venules), and the venous system. See Figure 1. The pulmonary vascular bed has similar components, but the properties of the pulmonary vascular resistance are unique.

Figure 1



We will assume that the major resistive component in the systemic circulation is located at the level of the microcirculation (primarily the arterioles), and that the large arteries and veins contribute primarily capacitance. We will include, however, a small resistance in the venous return path. The venous capacitance is much larger than that of the arteries and provides the major reservoir for blood volume.

B. Vascular Resistance

Laminar viscous flow in rigid tubes (Poiseuille flow) results in a parabolic distribution of velocities across the tube, and a linear relationship exists between the pressure drop, P , and the flow rate, Q , through the tube.

$$\Delta P = RQ \quad (1)$$

The constant of proportionality is the resistance to flow, R . It is dependent upon the geometry of the tube and the viscosity, μ , of the fluid.

$$R = \frac{8}{\pi} \mu \frac{l}{r^4} \quad (2)$$

where l is the length of the tube over which ΔP is measured, and r is the radius of the tube. If the flow is measured in cc/sec, and ΔP in dynes/cm², then the units of resistance are dyne-sec/cm⁵. If pressure is measured in mmHg and flow in cc/sec., resistance is expressed in “peripheral resistance units,” or PRU. Note that if the mean pressure drop across the circulation were 80 mmHg and the cardiac output were 5 liters/min. (which is about 80 cc/sec.) then total peripheral resistance would be close to 1 PRU.

The resistance of the tube is directly proportional to length and viscosity and inversely proportional to the fourth power of the radius. Thus, one would expect that the major contribution to vascular resistance would be made by the smallest vessels.

One may use the measured flow distribution in the various vascular beds and the Poiseuille formula to estimate the relative resistance offered by various vessels. Such estimates are contained in Table 1, confirming that arterioles are the site of most of the peripheral resistance.

Table 1
Relative Resistance to Flow in the Vascular Bed

Aorta	4%	Venules	4%
Large arteries	5%	Terminal Veins	0.3%
Mean arterial branches	10%	Main venous branches	0.7%
Terminal branches	6%	Large veins	0.5%
Arterioles	41%	Vena cava	1.3%
Capillaries	27%		
Total: arterial + capillary = 93%		Total venous = 7%	

(From Burton 1972, p. 91)

Note also that the strong dependence of the resistance upon vessel radius implies that sensitive regulation of flow is possible by changes in vessel diameter due to smooth muscle action.

Although Poiseuille's law has many engineering applications, and although it gives considerable insight into flow in the circulation; nevertheless, it cannot be rigorously applied to the circulation. It requires the following assumptions:

i) **The fluid is homogeneous and Newtonian.**

Blood may be considered as a Newtonian fluid only if the radius of the vessel exceeds 0.5 mm, and if the shear rate exceeds 100 sec^{-1} . This condition, therefore excludes arterioles, venules, and capillaries, since they are generally considerably less than 1 mm in diameter.

ii) **The flow is steady and inertia-free.**

If the flow is pulsatile, the variable pressure gradient communicates kinetic energy to the fluid, and the flow is no longer inertia-free. This condition excludes the larger arteries.

iii) **The tube is rigid so that its diameter does not change with pressure.**

This condition is never met in the circulatory system. The veins in particular depart from this assumption.

Although Poiseuille's law does not apply strictly, we will consider that pressure and flow are linearly related in those parts of the circulation in which the viscous forces predominate over inertial forces (low Reynolds numbers). Hence, we will represent the small vessels (arterioles, capillaries, and venules) as linear resistance elements governed by Eq. 1. (The calculation of R may require modification in some vascular beds, however.)

C. Vascular Capacitance

1. Introduction

The walls of blood vessels are not rigid, but rather they stretch in response to increased transmural pressure. The vessel walls contain four major elements: endothelial lining, elastin fibers, collagen fibers, and smooth muscle. The endothelium provides a smooth wall, and offers selective permeability to certain substances. The endothelial cells play very little part in the total elasticity of the walls. However, endothelial cells are active sensors of fluid shear stresses, and play an important role in regulation of smooth muscle tone via release of vasoactive molecules. The

elastin fibers are easily stretched (about six times more easily than rubber). They produce an elastic tension automatically as the vessel expands, and without biochemical energy expenditure. The collagen fibers are much stiffer than the elastin fibers. However, these fibers are slack, and do not exert their tension until the vessel has been stretched. Thus, the more the vessel expands, the stiffer it becomes. The smooth muscle serves to produce an *active* tension, contracting under physiological control, and changing the diameter of the lumen of the vessel. Figure 2 shows the relative mixtures of the four elements in walls of various vessels. Notice the predominance of elastin in the large and medium arteries, and the predominance of smooth muscle in the small arterioles. The former are elastic “storage” vessels, while the latter are controllable “resistance” vessels. The thin-walled collapsible veins perform the major storage, or capacitance role in the circulation. The capillaries are formed of only a one cell thick endothelium, and are well suited for their role as an exchange mechanism between the circulating blood and the interstitial fluid.

Figure 2

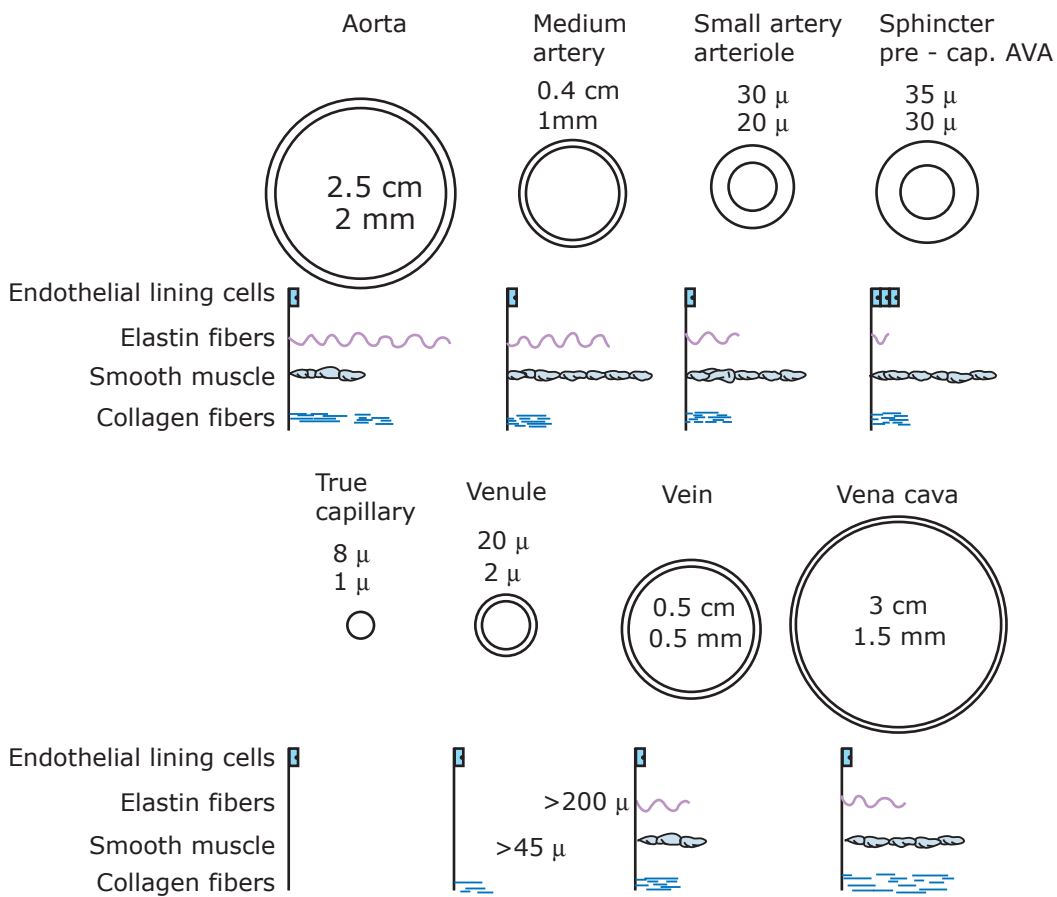


Figure by MIT OCW. After p. 64 in Burton. *Physiology and Biophysics of the Circulation*. Chicago: Year Book Medical Publishers, 1972.

Variety of size, thickness of wall and admixture of the four basic tissues in the wall of different blood vessels. The figures directly under the name of the vessel represent the diameter of the lumen; below this, the thickness of the wall. *End.*, endothelial lining cells. *Ela.*, elastin fibers. *Mus.*, smooth muscle. *Fib.*, collagen fibers. (From Burton 1972, p. 64.)

As transmural pressure increases, blood vessels expand, store more volume, and hence behave as capacitance elements in the circulation. Volume-pressure curves for arteries and veins are shown in Figure 3. (Note the different scales.) The slope of the curve at any particular point is a measure of the incremental capacitance of the vessel. Notice that the V-P curves are not linear and that the vessels get stiffer as they expand—hence the incremental capacitance decreases. Note also that veins have a *much* larger capacitance than arteries, and are the major storage elements in the circulation.

$$C = \frac{\Delta V}{\Delta P} \quad (3)$$

Figure 3

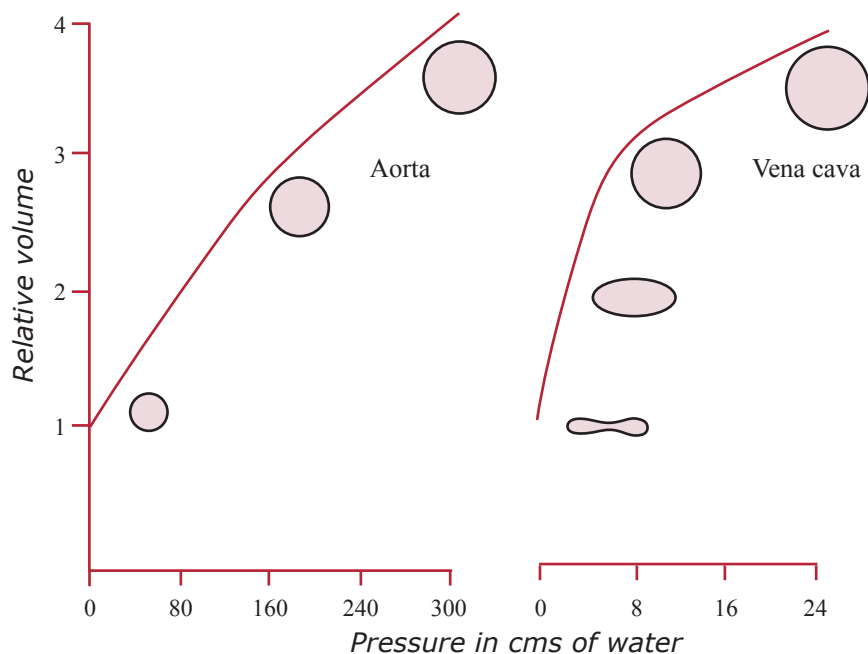


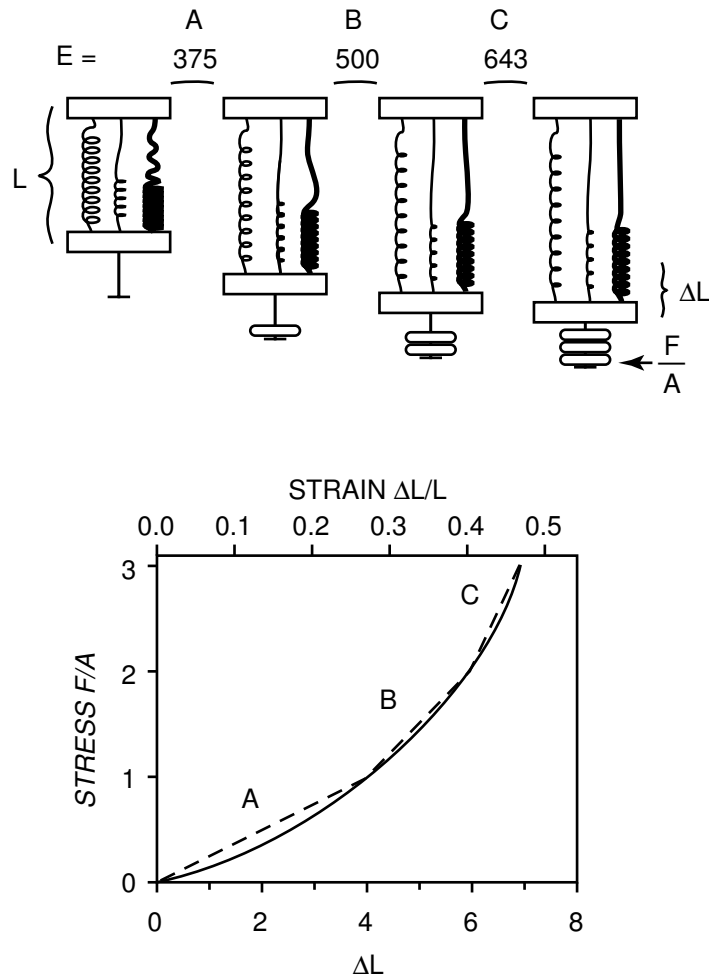
Figure by MIT OCW. After p. 55 in Burton. *Physiology and Biophysics of the Circulation*. Chicago: Year Book Medical Publishers, 1972.

Comparison of the distensibility of the aorta and of the vena cava. The way in which the cross-section of the vessels changes in the two cases is also indicated. (From Burton 1972, p. 55.)

The model shown in Figure 4 provides an explanation for the non-linear behavior. In the figure, the thin coils represent “weak” elastin fibers at different lengths. The heavy coil represents a “stiff” collagen fiber which is initially not under tension. As the material is stretched, more parallel springs are added, which increase overall stiffness as distension is increased. It is also true that the capacitance of arteries decreases with age. This increase in stiffness may be due to an

increased resting length of the elastic and collagen fibers, so a greater number of fibers would be stretched in parallel; or to changes in the amount of collagen in the vessel walls.

Figure 4



Model explaining the increase in elastic modulus (E) which develops at high strains ($\Delta L/L$). Stress (F/A) is portrayed by weights which are added to the lower bar. Light springs represent elastin fibers, and the heavy spring represents a collagen fiber.

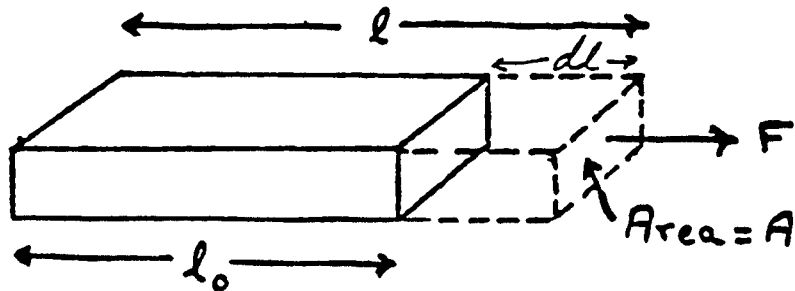
2. Calculation of Vascular Capacitance

a. Hooke's Law

Consider a strip of material of length l_0 , and cross-sectional area, A . (See figure 5.) The material is in equilibrium with a force F_0 applied to it. The equilibrium tensile stress then is $\sigma = F_0/A$. If the stress is increased to $\sigma + d\sigma'$, the length will increase to $l_0 + dl$. *Hooke's Law* relates the fractional change in length dl/l_0 (the strain) to the change in stress, $d\sigma$.

$$d\sigma = E \frac{dl}{l_0} \quad (4)$$

Figure 5



The constant, E , is known as Young's modulus. The larger E , the "stiffer" the material. For blood vessels, E is not constant, but is a function of pressure. The following table shows the variation of E with transmural pressure for the thoracic aorta.

Table 2
Variation of Young's Modulus with Intraaortic Pressure

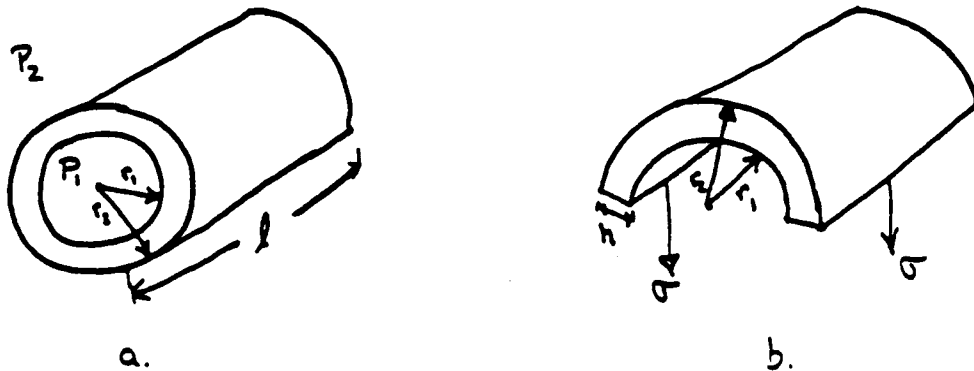
P, mmHg	E, dynes/cm ² x 10 ⁶
60	1.2
100	4.2
160	10
220	18
Note: 1 mmHg = 1330 dynes/cm ²	

b. LaPlace's Law

It is often of importance to relate the tension in the walls of hollow vessels to the transmural pressure across the walls. Consider a cylinder of length, l , and wall thickness h (Figure 6a). The inner radius is r_1 and the outer radius is r_2 . The internal pressure is p_1 , and the external pressure is p_2 . The wall stress (force per unit area) is σ . We wish to derive the relation between σ and the transmural pressure. Imagine that the cylinder is split down the axis (Figure 6b). The total force pulling the cylinder half down will be:

$$F_1 = 2\sigma h l$$

Figure 6



Opposing this force will be that due to the pressures acting on the projected area of the cylindrical walls. The net force due to the pressure differences is:

$$F_2 = 2P_1r_1l - 2P_2r_2l$$

In order to have equilibrium,

$$\begin{aligned} F_1 &= F_2 \\ 2\sigma h l &= 2l(P_1r_1 - P_2r_2) \\ \sigma h &= (P_1r_1 - P_2r_2) \end{aligned}$$
(5)

If the vessel is thin-walled ($h \ll r$), then $r_1 \approx r_2 = r_0$ and

$$\sigma h = r_0 P \quad (6)$$

where P is the transmural pressure. Equation (6) is an expression of LaPlace's law for a thin-walled cylinder. Note that for a given transmural pressure, the wall tension ($T = \sigma h$) per unit length increases as the radius increases and vice versa.

Can you derive Laplace's law for a thin-walled sphere? $\left(\sigma h = \frac{r_0 P}{2} \right)$

c. Calculation of Arterial Capacitance

The arterial capacitance per unit length, C_u , may be calculated assuming that vessel length does not vary with transmural pressure.

$$C_u = \frac{dA(p,x)}{dP(x)} \quad (7)$$

where $A(p,x)$ and $P(x)$ are the vessel cross-sectional area and transmural pressure respectively. Both may be functions of x , the length along the vessel axis, and the area will also vary with pressure, P .

From LaPlace's Law (Eq. 6) we may relate the change in wall stress to the change in transmural pressure at a particular radius, r_0 .

$$d\sigma = \frac{r_0}{h} dP + \frac{P}{h} dr \quad (8)$$

From Hooke's law we have

$$d\sigma = E \frac{dc}{c_0} \quad (9)$$

where c is the circumference of the cylinder, $2\pi r$.

$$d\sigma = E \frac{2\pi dr}{2\pi r_0} = E \frac{dr}{r_0} \quad (10)$$

Combining (8) and (10) we obtain the relation between changes in radius and changes in pressure

$$\frac{dr}{dP} = \frac{\frac{r_0}{h}}{\left(\frac{E}{r_0} - \frac{P}{h} \right)} \quad (11)$$

From (7):

$$C_u = \frac{dA}{dP} = \frac{d(\pi r^2)}{dP} = 2\pi r_0 \frac{dr}{dP} \quad (12)$$

$$C_u = \frac{2\pi r_0^2}{\left(\frac{Eh}{r_0} - P \right)} \quad (13)$$

In most situations the denominator may be simplified by neglecting P , since $\frac{Eh}{r_0}$ is the dominant term. For example, if $\frac{h}{r_0} \approx 0.1$ and $E = 10^7$

$$\frac{Eh}{r_0} \approx 10^6 \text{ dynes/cm}^2$$

$$P \approx 100 \text{ mmHg} = 133,000 \text{ dynes/cm}^2$$

So,

$$C_u \approx \frac{2\pi r_0^3}{Eh}$$

3. Electrical/Mechanical Analysis

It is often useful to use electrical analogies and symbols for fluid variables. A table of such corresponding variables is presented in Table 3 below.

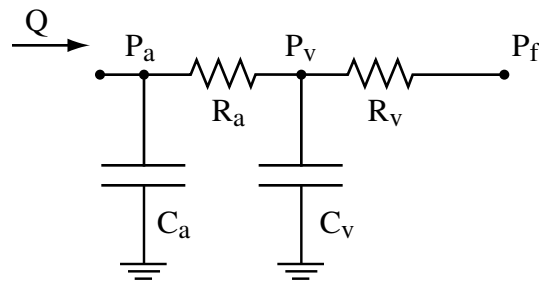
Table 3

Fluid Variable	Electrical Variable
Pressure, P	Voltage, e
Flow, Q	Current, i
Volume, V	Charge, q
Resistance, $R = \Delta P/Q$	Resistance, $R = \Delta e/i$
Capacitance, $C = \Delta V/\Delta P$	Capacitance, $C = \Delta q/\Delta e$

D. A Lumped Parameter Model of the Peripheral Circulation

Figure 7 represents the same circulatory segment as Figure 1 using electrical symbolism:

Figure 7



In the figure, C_a represents the equivalent capacitance of the arteries, and C_v the total capacitance of all the veins in the circulation under consideration. R_a is the “peripheral” resistance, and R_v the resistance to venous flow. Q is the mean flow rate, P_a the arterial transmural pressure, P_v the venous transmural pressure, and P_f the right atrial or “filling” pressure.

Typical values for each of the components for an adult human are as follows:

Table 4
Representative Values for Lumped Parameter Model

$C_a = 2 \text{ ml/mmHg}$
$C_v = 100 \text{ ml/mmHg}$
$R_a = 1 \text{ mmHg/ml/sec.}$
$R_v = .06 \text{ mmHg/ml/sec.}$

We now proceed to an analysis of the model of Figure 7. Specifically, we would like to establish the relationship between the mean flow rate through the vasculature, Q , and the right atrial filling pressure, P_f . The reasons for the choice of these parameters will become clearer after discussing ventricular function, but it is obvious that we could equally well choose other variables to relate if desired.

We will designate by V_t the total volume of blood in the peripheral circulation. This represents approximately 85% of the total blood volume. The remaining fifteen percent resides in the heart and pulmonary circulation. Of the total blood volume in the peripheral circulation, an amount V_0 is required just to fill the undistended system before any transmural pressure is

developed. V_0 is known as the “zero-pressure filling volume”, or the “non-stressed volume”. The pressure-volume relationships of the arterial and venous systems are plotted below in Figure 8. The figure also shows the effects of varying amounts of sympathetic nervous tone. (Increase in sympathetic tone causes vascular smooth muscle to contract, thus shrinking the size of blood vessels.)

Figure 8

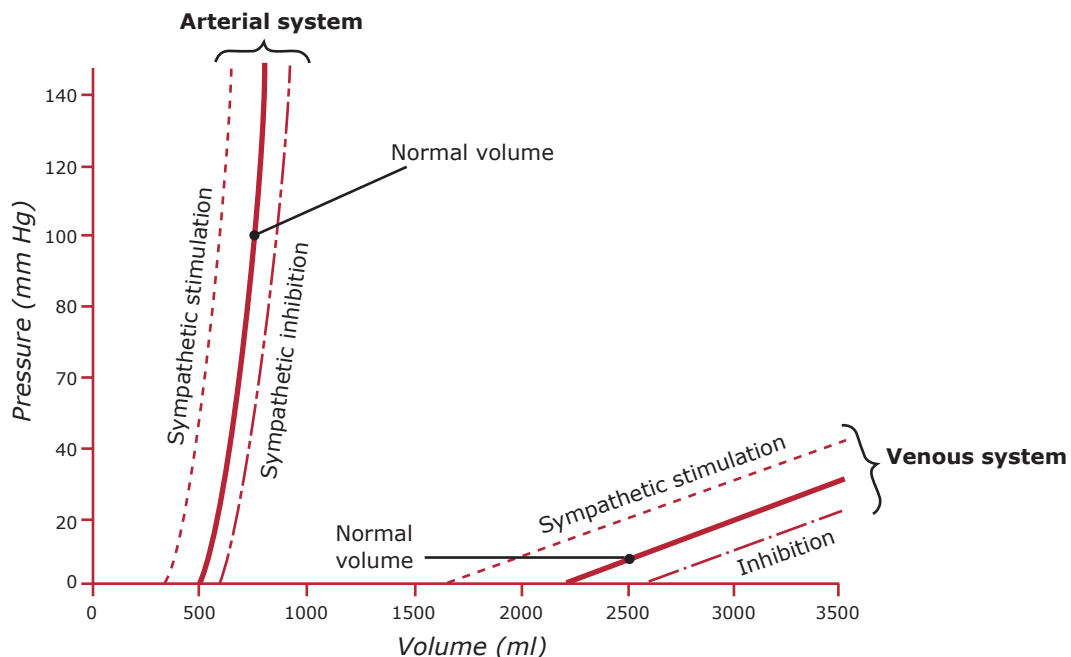


Figure by MIT OCW. After Guyton. *Human Physiology and Mechanisms of Disease*. 3rd ed. Philadelphia: W.B. Saunders, 1982.

The volumes stored in the arterial and venous capacitances are given by

$$V_a = C_a P_a + V_{a0} \quad (14)$$

$$V_v = C_v P_v + V_{v0} \quad (15)$$

The total blood volume in the peripheral circulation is fixed at V_t ,

$$V_t = V_a + V_v = C_a P_a + C_v P_v + V_0 \quad (16)$$

V_0 is on the order of 3,000 ml in the adult (500 cc. in V_{a0} , and 2500 cc. in V_{v0}). V_t is approximately 4,000 ml. During each cardiac cycle, a stroke volume ΔV enters the arterial system and an equal quantity leaves the peripheral vasculature through the venous system to enter the right heart. ΔV is small compared to $V_t - V_0$. ($\Delta V \approx 80$ cc.)

In steady state if the mean flow is Q , then there will be a pressure drop across each resistance such that

$$P_a - P_v = QR_a \quad (17)$$

$$P_v - P_f = QR_v \quad (18)$$

Suppose the flow were to go to zero. Now all the pressure gradients would disappear, the volume would adjust itself in arteries and veins accordingly, and there would be a *mean systemic filling pressure*, P_{ms} , observed at all points.

$$P_a = P_v = P_f = P_{ms}$$

Since now both capacitances are at the same pressure, we have:

$$\begin{aligned} V_a &= C_a P_{ms} + V_{a0} \\ V_v &= C_v P_{ms} + V_{v0} \end{aligned}$$

and

$$V_t = P_{ms}(C_a + C_v) + (V_{a0} + V_{v0}) \quad (19)$$

Note that

$$P_{ms} = \frac{V_t - (V_{a0} + V_{v0})}{C_a + C_v} = \frac{V_t - V_0}{C_t} \quad (20)$$

where C_t is the total capacitance of both arteries and veins. Thus P_{ms} is an **intrinsic** property of the vascular network provided the blood volume and vascular capacitance (vascular tone) are kept constant. **P_{ms} is the ratio of total distending volume ($V_t - V_0$) to total systemic capacitance.**

We will now derive an expression relating the flow, Q , to the filling pressure, P_f and the mean systemic filling pressure P_{ms} .

From Eqs. (17) and (18) or from inspection of the circuit we have:

$$Q = \frac{P_a - P_f}{R_a + R_v} \quad (21)$$

P_a may be related to P_{ms} by combining eqs. (16) and (20)

$$C_a P_a + C_v P_v = P_{ms}(C_a + C_v)$$

Using eq. (17), we have:

$$\begin{aligned} C_a P_a + C_v (P_a - QR_a) &= P_{ms}(C_a + C_v) \\ P_a(C_a + C_v) - QR_a C_v &= P_{ms}(C_a + C_v) \\ P_a &= P_{ms} + QR_a \frac{C_v}{C_a + C_v} \end{aligned} \quad (22)$$

Substituting (22) into (21) and rearranging, we obtain:

$$Q = \frac{P_{ms} - P_f}{R_v + R_a \left(\frac{C_a}{C_a + C_v} \right)} \quad (23)$$

Equation (23) relates flow to filling pressure and includes P_{ms} (a basic property of the system) and the R_s and C_s . From the table of representative values given in Table 4 above it can be seen that the second term in the denominator is the same order of magnitude as the first term.

It should be noted that if P_f is lowered below atmospheric pressure, the veins entering the thorax will collapse. Hence, venous return to the heart cannot be increased by negative filling pressures. (This is the same phenomenon as trying to suck fluid up through a collapsible straw. The collapse of veins is readily observed in the neck veins, and the veins on the dorsum of the hands.) The venous return at 0 mmHg tends to be maintained for $P_f \leq 0$.

As early as 1914, Starling (Patterson and Starling 1914) made use of the collapse phenomenon in his isolated heart-lung preparation (“Starling resistors”). The first theoretical and experimental studies of flow through collapsible tubing were done by Holt (1941, 1969). He used the apparatus shown below (Figure 9a), and measured the flow, Q , through a section of collapsible tube as a function of the pressure just proximal to the segment (P_1), the pressure just distal to the segment (P_2), and the pressure external to the segment, P_e . A typical experimental result is shown

in Figure 9b, which relates flow to P_2 when P_e and P_1 are held constant. For downstream pressures exceeding the external pressure ($P_2 > P_e$) the vessel is open throughout its length, and the slope of the line is determined by the flow resistance of the open cylindrical tube. For downstream pressures less than the external pressure, the flow is independent of P_2 , and is determined by $P_1 - P_e$. (For more discussion of flow through collapsible tubes, see Caro et al. 1978, 460ff, or Fung 1984, 186ff).

Figure 9

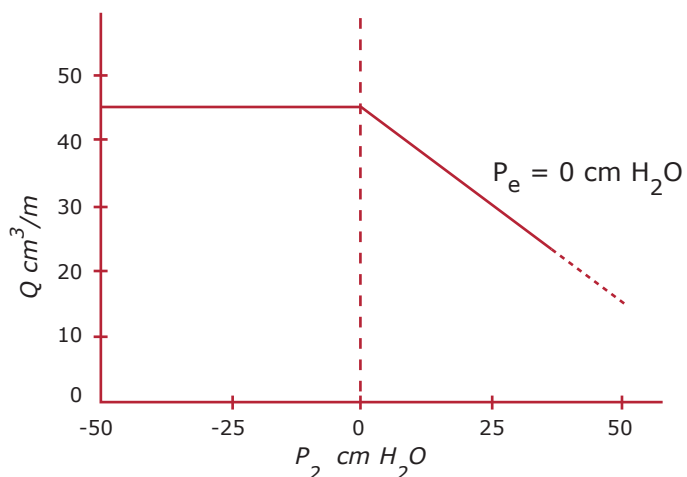
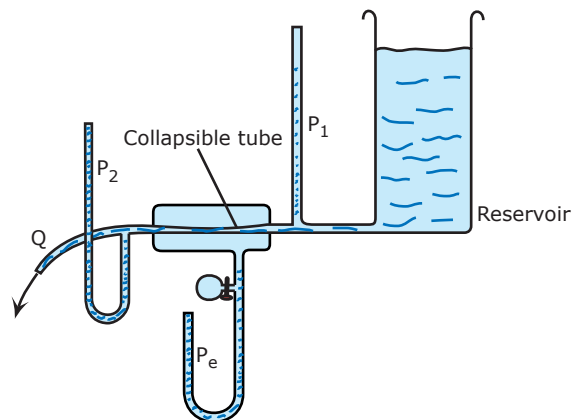
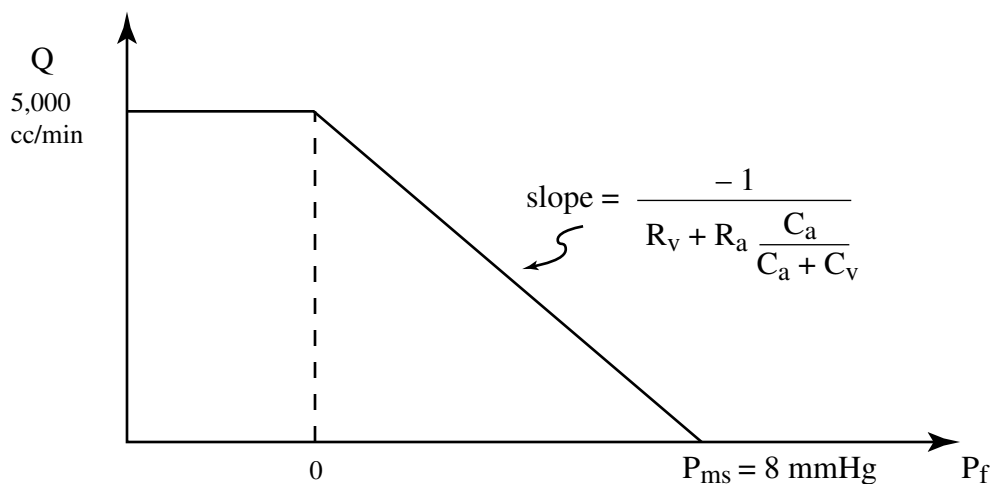


Figure by MIT OCW. After Noordergraaf. *Circulatory System Dynamics*. New York: Academic Press, 1978, p. 162.

Diagram of Holt's experimental set-up (1941) to investigate flow in collapsible tubes. P_1 denotes pressure just upstream of the collapsible tube; P_2 pressure just downstream; P_e is the pressure external to the collapsible tube. Q stands for flow. (b) Flow in a segment of Penrose tubing as a function of downstream pressure with P_e equal to atmospheric pressure and reservoir-height constant. (From Noordergraaf 1978, p. 162.)

Figure 10
The Venous Return Curve



A graphical representation of equation (23) is shown in Figure 10. This plot of total flow versus P_f was termed the “venous return curve” by Dr. Arthur Guyton, and is extensively used in his graphical analysis (Guyton 1973). The following figures illustrate the effects on the flow rate of manipulating various parameters: (All experimental curves are for dogs, and idealized curves are for humans.)

1. Changing Resistance

The slope of the venous return curve may be changed by varying the quantity $\left[R_v + R_a \frac{C_a}{C_a + C_v} \right]$. Thus, interventions that change peripheral resistance, R_a , or the venous return resistance R_v (such as compressing the large veins) will cause *only* a slope change (Figs. 11 and 12 show idealized human curves, and actual experimental data from dogs.)

Figure 11
(Idealized curves for humans)

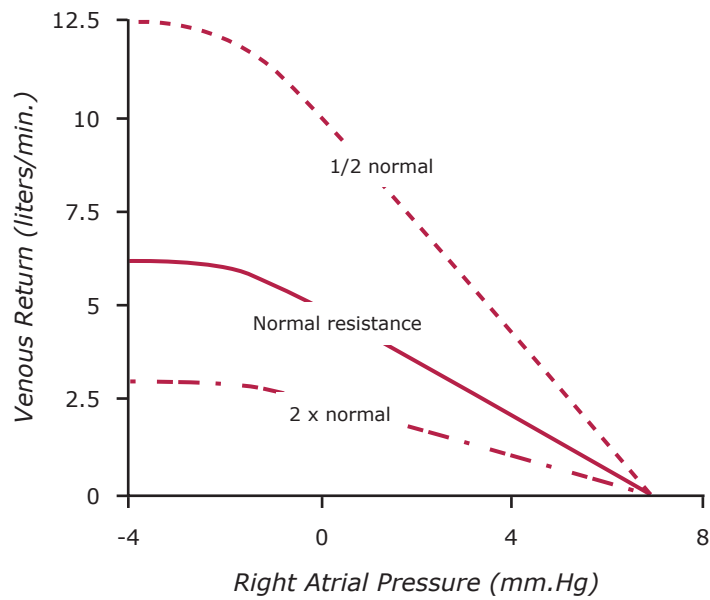


Figure by MIT OCW. After Guyton (1973), Fig. 13-1.

Calculated effects on the venous return curve caused by a two fold increase or a two fold decrease in total peripheral resistance when the resistances throughout the systemic circulation are all altered proportionately. (Guyton 1973, p. 223.)

Figure 12
(Experimental data from dogs)

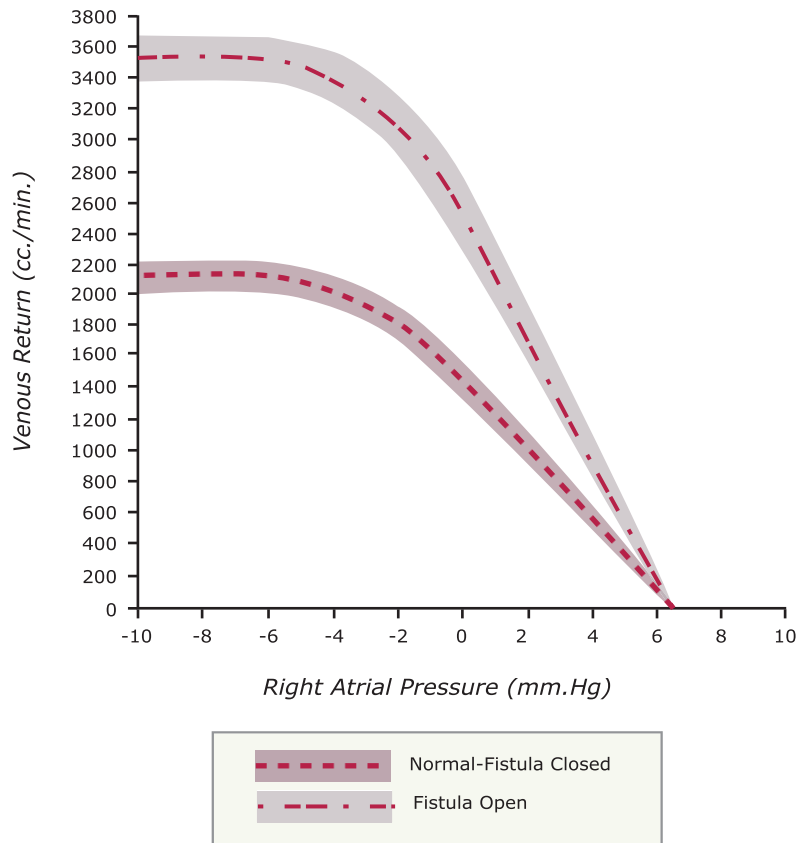


Figure by MIT OCW. After Guyton (1973), Fig. 13-2.

Average effect on the venous return curve in 10 areflexic dogs of opening a large A-V fistula. Shaded areas indicate probable errors of the means. (Guyton 1973, p. 225.)

2. Changing mean systemic filling pressure. (How might this be done?)

The mean systemic filling pressure determines the x-intercept of the venous return curves, but does not alter the slope. P_{ms} may be altered by manipulating either the total blood volume stored in the peripheral circulation or the zero-pressure filling volume of the veins. See Figures 13 and 14.

Figure 13

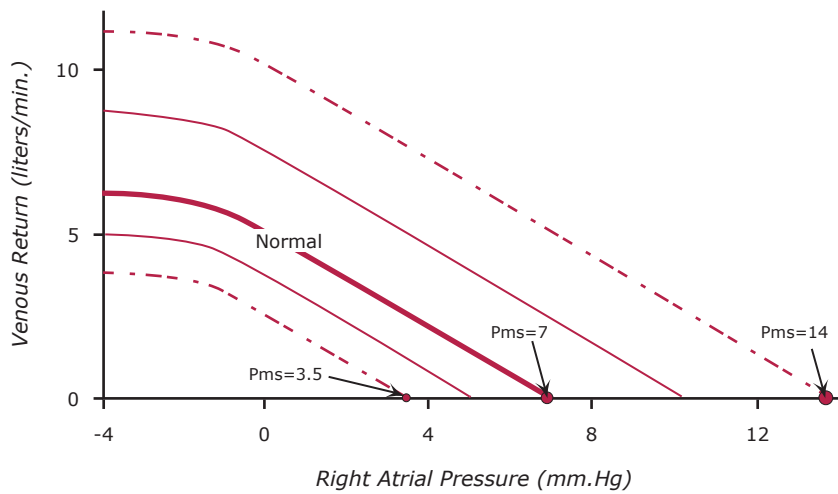


Figure by MIT OCW. After Guyton (1973), Fig. 14-5.

Idealized curves, showing the effect on the venous return curve caused by changes in mean systemic filling pressure. (Guyton 1973, p. 243.)

Figure 14
Changing P_{ms} by manipulating venous smooth muscle tone

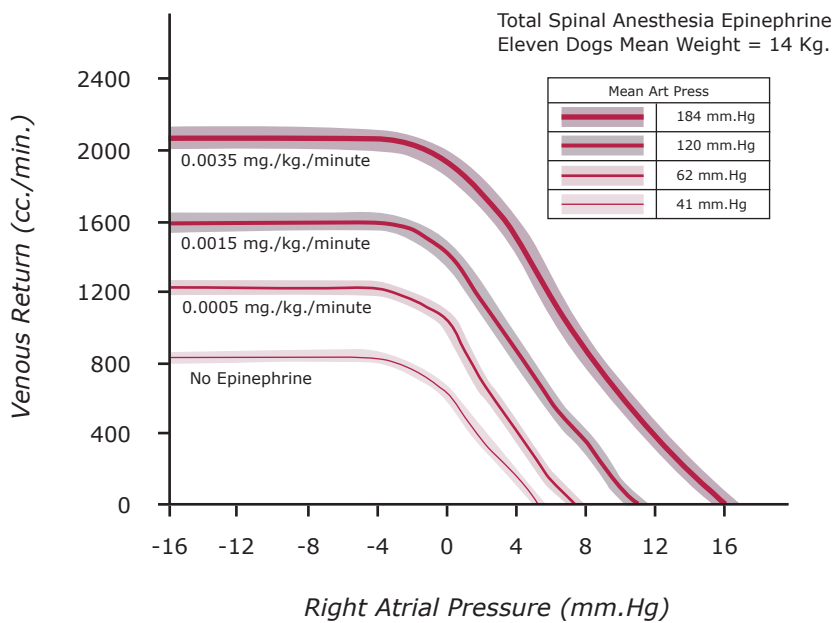


Figure by MIT OCW. After Guyton (1973), Fig. 12-10.

The animals used in these studies had total spinal anesthesia to remove all circulatory reflexes, and the curves are mean values from 11 dogs averaging 14 kg. weight. The shaded areas indicate the probably errors of the means. (Guyton 1973, p. 218.)

Figure 15
Changing mean systemic filling pressure by manipulation of blood volume

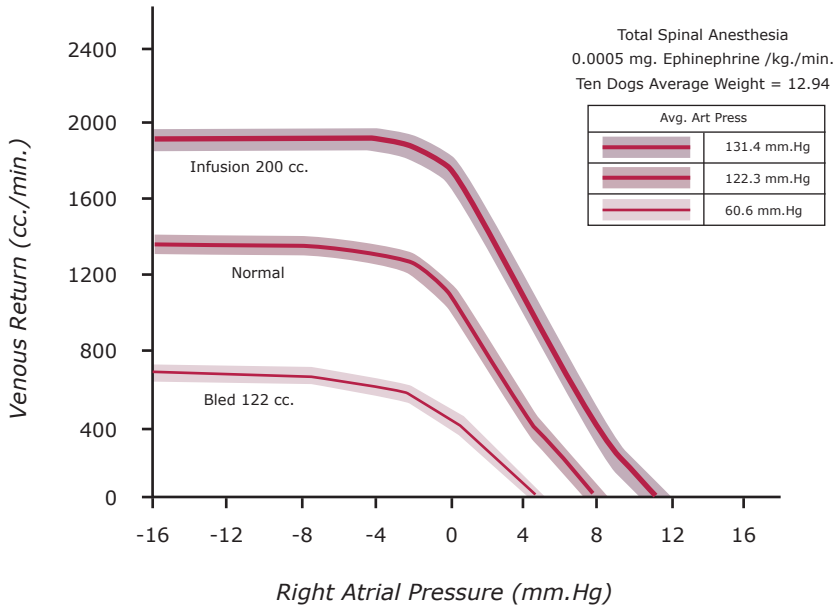


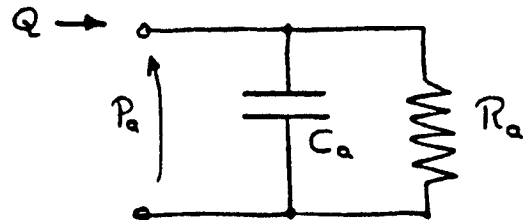
Figure by MIT OCW. After Guyton (1973), Fig. 12-7.

Average venous return curves recorded in 10 dogs, showing (a) the average normal curve, (b) the average curve after bleeding the animals an average of 122 ml. of blood, and (c) after returning the removed blood and infusing an additional 200 ml. of blood. These animals were given total spinal anesthesia and a continuous infusion of epinephrine to cause (1) abrogation of all circulatory reflexes and (2) maintenance of the vasomotor tone at a normal level. (Guyton 1973, p. 215)

E. The Windkessel Simplification

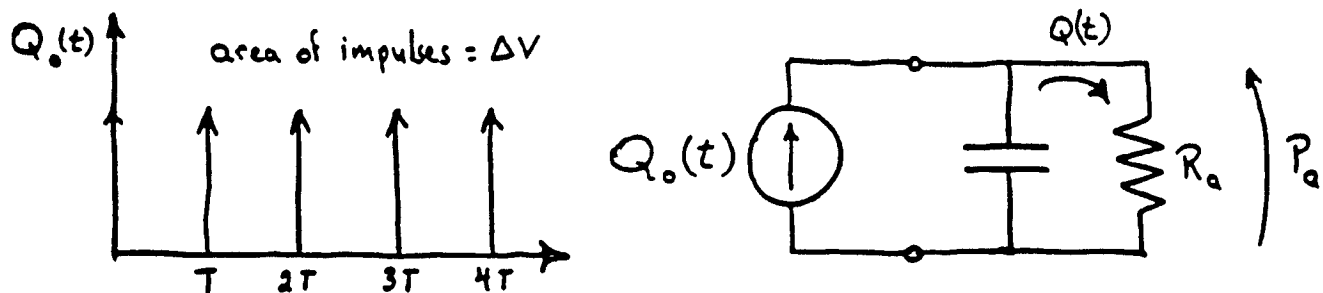
If we restrict our attention to the flow and pressure in the aorta, we may simplify the model of the peripheral circulation by assuming that the venous pressure is constant and approximately zero ($P_v = 0$). Our model then reduces to that shown in Figure 16. This simple model is known as the Windkessel model.

Figure 16



It was originally proposed by the German physicist, O. Frank (Frank 1888). It is a simplified model which represents the circulation as a compliant system of major vessels in which negligible frictional losses are present, and a terminal vascular resistance (the microcirculation). It is instructive here to discuss the expected behavior of the simple Windkessel model for the peripheral circulation if it is driven with a “heart” modelled as a periodic flow impulse generator that ejects stroke volumes of ΔV . (See Figure 17.)

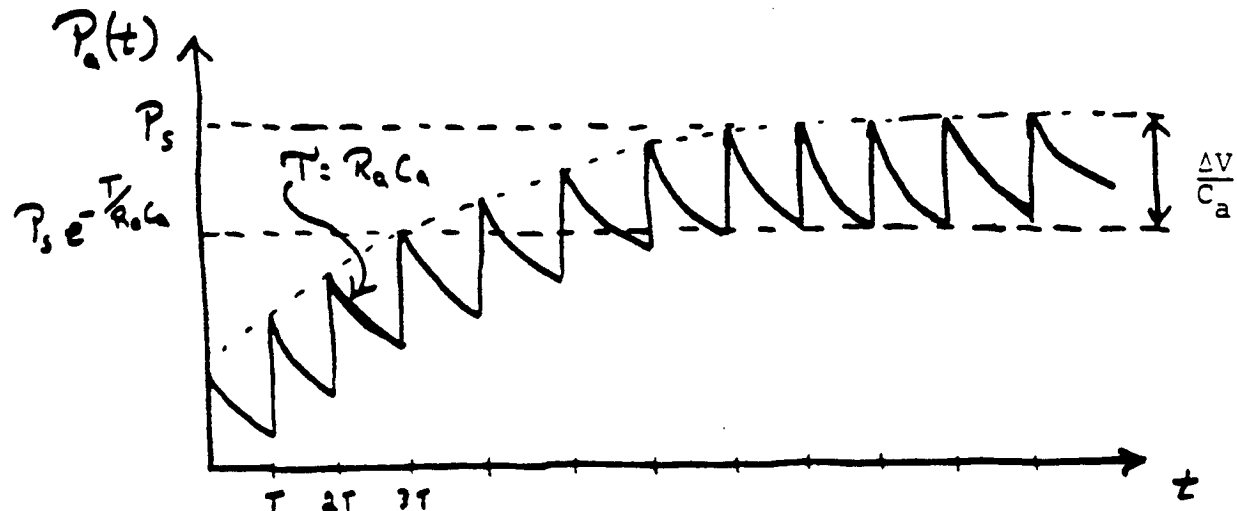
Figure 17



Using this model, it is possible to express the arterial pressure (systolic, diastolic, and mean) in terms of the model parameters, and to observe the dependence of these pressures on stroke volume, heart rate, arterial capacitance, and peripheral resistance.

If the system starts at $t = 0$ with no volume in the capacitance vessels, the pressure waveform will build up over time as shown in Figure 18.

Figure 18



The initial stroke volume will be instantaneously deposited in the arterial capacitance, and arterial pressure will rise by $\Delta V/C_a$. The pressure will then decay exponentially, with a time constant $\tau = R_a C_a$ as the volume leaves the capacitor through the peripheral resistance, R_a . Before the pressure reaches zero the next impulse of volume is “dumped” into the capacitor, again raising the pressure by an amount $\Delta V/C_a$. Eventually the system will reach equilibrium when the volume deposited in the capacitance per beat is exactly matched by the volume leaving the capacitor through the peripheral resistance. We may make use of this requirement of equilibrium to solve the system for the maximum, minimum, and mean arterial pressures in terms of the stroke volume, ΔV , the time between impulses, T , and the properties of the circulation, R_a and C_a .

In steady state, the increment in pressure corresponding to the sudden dumping of ΔV onto C_a will be $\Delta V/C_a$. In the time, T , during which C_a discharges exponentially through R_a , the pressure must drop an equal amount.

If the steady-state peak pressure is P_s (systolic pressure), the minimal (diastolic) pressure T seconds later would be

$$P_d = P_s e^{-T/R_a C_a}$$

Hence, the pressure decrease would be

$$P_s \left(1 - e^{-T/R_a C_a}\right)$$

Setting this quantity equal to $\Delta V/C_a$, we have:

$$P_s \left(1 - e^{-T/R_a C_a}\right) = \frac{\Delta V}{C_a} \quad (24)$$

Thus, systolic pressure is given by:

$$P_s = \frac{\Delta V}{C_a} \cdot \frac{1}{\left(1 - e^{-T/R_a C_a}\right)} \quad (25)$$

During the intervals, $nT < t < (n + 1)T$, the expression for arterial pressure then becomes

$$P_a(t) = \frac{\Delta V}{C_a} \cdot \frac{e^{-(t-nT)/R_a C_a}}{\left(1 - e^{-T/R_a C_a}\right)} \quad (26)$$

Diastolic Pressure

$$P_d = \frac{\Delta V}{C_a} \cdot \frac{e^{-T/R_a C_a}}{(1 - e^{-T/R_a C_a})} \quad (27)$$

Pulse Pressure

$$P_s - P_d = \frac{\Delta V}{C_a} \quad (28)$$

The mean pressure P_a is simply the product of the average flow, $\Delta V/T$, and the resistance, R_a . Thus:

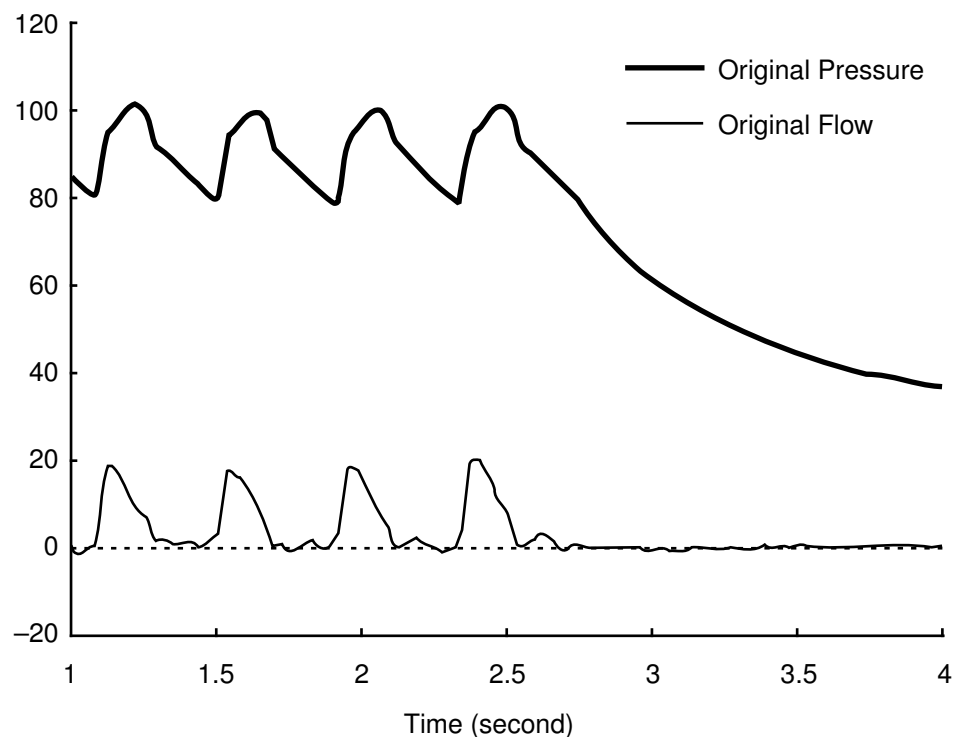
$$\begin{aligned} P_a &= \frac{\Delta V}{T} \cdot R_a \\ &= \frac{\Delta V}{60} \cdot f \cdot R_a \quad (f \equiv \text{beats per minute}) \end{aligned} \quad (29)$$

Several points are worth observing from the above expressions—first, the mean arterial pressure is directly proportional to heart rate, stroke volume, and peripheral resistance, as would be expected. Since stroke volume times heart rate equals cardiac output, Equation (29) simply states that the mean arterial pressure equals the product of cardiac output and peripheral resistance.

Examination of Equation (28) reveals that the pulse pressure is directly proportional to the stroke volume and inversely proportional to arterial capacitance. What does this imply for patients with severe arteriosclerotic vascular disease with pipe-like arteries? Does it suggest a simple approximate technique to monitor stroke volume?

The exponential decay during diastole is a realistic representation of the pressure in the human aorta. Using our typical values of $R_a \approx 1 \text{ mmHg/ml/sec}$. and $C_a \approx 2 \text{ ml/mmHg}$, the time constant for the decay is about 2 sec. Figure 19 shows the intrarterial blood pressure and flow measured in the rabbit aorta. At $t = 2.5 \text{ sec}$. the heart is stopped with vagal stimulation, and the blood pressure falls exponentially, consistent with the Windkessel model.

Figure 19



II. THE HEART AS A PUMP

A. Introduction

The performance of the heart as a pump is dependent primarily upon the contraction and relaxation properties of the heart muscle cells (myocardium). Other factors must also be considered such as: the geometric organization of these cells, the presence of connective tissue, the heart's electrical rhythm, and valve function. In this section we will examine the mechanical function of the intact heart and its cellular basis. We will then present a simple model for the heart-pump and explore the interaction between the heart and peripheral circulation.

The heart is a hollow chamber whose walls consist of a mechanical syncytium of myocardial cells. Figure 20 shows the structure of the myocardium at various levels of detail. Notice that cardiac muscle is very similar in structure to skeletal muscle, particularly with regard to the sarcomere organization.

1. The Length-Tension Relationship

The biochemical events leading to contraction are similar in skeletal and cardiac muscle. The theory most generally accepted is the sliding filament hypothesis, in which contractile force is developed as cross-bridges form between thick and thin filaments in the sarcomeres. Calcium is the trigger for this process as it is released into the cell cytoplasm following an action potential. Relaxation of the muscle occurs as calcium is actively removed from the region of the contractile apparatus by the sarcoplasmic reticulum. (Students who are not familiar with muscle physiology should read chapters 17-18 of Berne and Levy. The biochemical details of electrical excitation-contraction coupling are reviewed in detail in Katz 1992 and Opie 1998, chapter 8.)

The total force generated by a contracting muscle is a function of the degree of overlap between thick and thin filaments, and hence contractile force will be a function of muscle length. The classical findings relating **skeletal** muscle length and developed tension are shown in Figure 21.

Figure 20 - Myocardial Structure

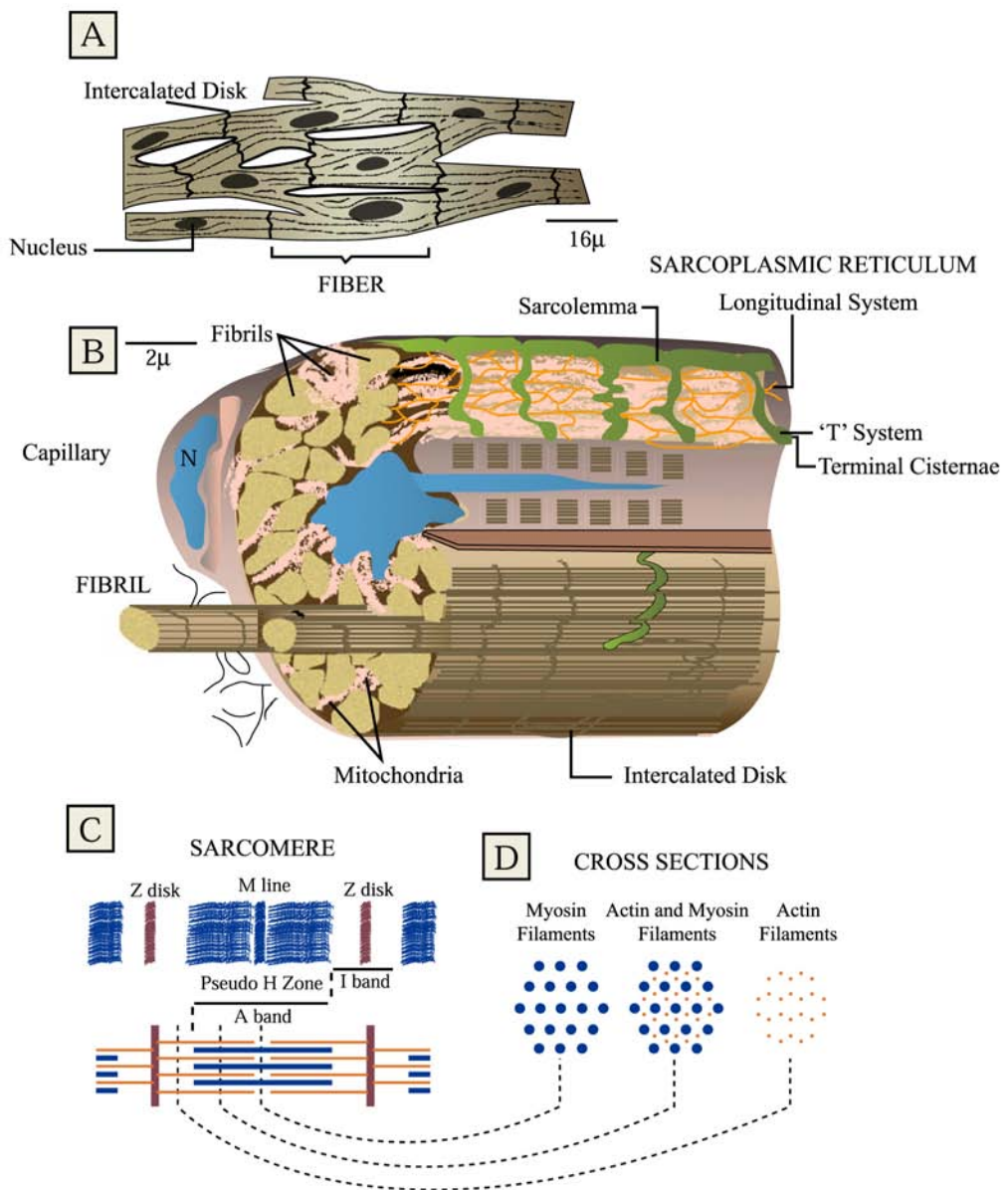


Figure by MIT OCW. After Braunwald, Ross, and Sonnenblick. *Mechanisms of Contraction in the Normal and Failing Heart*. 2nd ed. Little-Brown, 1976.

Myocardial structure, as seen under the light and electron microscopes, is schematized. Top drawing shows section of myocardium as it would appear under light microscope, with interconnecting fibers or cells attached end-to-end and delimited by modified cell membranes called intercalated disks. Ultrastructural schematization (center drawing) illustrates the division of the fiber longitudinally into rodlike fibrils, in turn composed of sarcomeres, the basic contractile units. Within the sarcomeres, thick filaments of myosin, confined to the central dark A band, alternate with thin filaments of actin which extend from the A lines (delimiting the sarcomere) through the I band and into the A band where they overlap the myosin filaments. These landmarks are seen in detail drawings (bottom). On activation a repetitive interaction between the sites shown displaces the filaments inward so that the sarcomere and hence the whole muscle shortens, with maximum overlap at 2.2μ . Also depicted are the membranous systems: the T system that carries electrical activity into the cells and the sarcoplasmic reticulum that releases calcium to activate the contractile machinery. Like the intercalated disks, these are specialized extensions of the superficial sarcolemma. Note also the rich mitochondrial content, typical of "red" muscle, which is highly dependent on aerobic metabolism. (From Braunwald, Ross, and Sonnenblick 1976).

Figure 21
Length-Tension Relationship in Skeletal Muscle

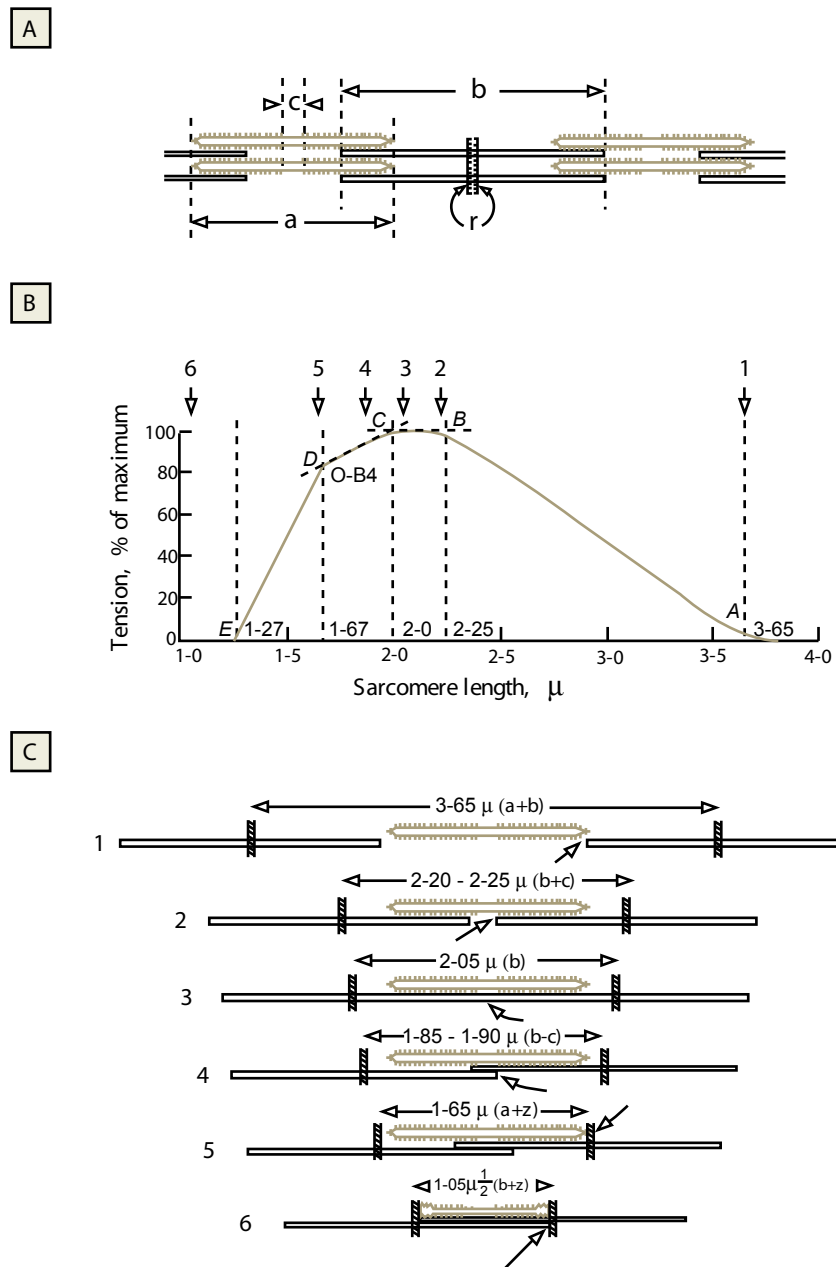


Figure by MIT OCW. After Braunwald, Ross, and Sonnenblick. *Mechanisms of Contraction in the Normal and Failing Heart*. 2nd ed. Little-Brown, 1976.

The relation between myofilament disposition and tension development in striated muscle. **A.** Diagram of the myofilament of the sarcomere drawn to scale. Thin filaments are 1.0μ and thick filaments 1.6μ in length. **B.** The relation between tension development (% of maximum) and sarcomere length in single fibers of skeletal muscle. The numbered arrows denote the breakpoints on the curve and correspond to the sarcomere lengths depicted in diagram form in C. **C.** Myofilament overlap shown as a function of sarcomere length. At 3.65μ (1) there is no overlap of myofilaments. The optimal overlap of myofilaments occurs at a sarcomere range of 2.05 to 2.25μ (between 2 and 3). At a sarcomere length shorter than 2.0μ (4) thin filaments pass into the opposite half of the sarcomere and a double overlap occurs (5 and 6). Note that the central 0.2μ of the thick filament is devoid of cross-bridges which could interact with sites on the think filaments. (From Braunwald, Ross, and Sonnenblick 1976).

Figure 22
Effect of Sarcomere Length on Tension

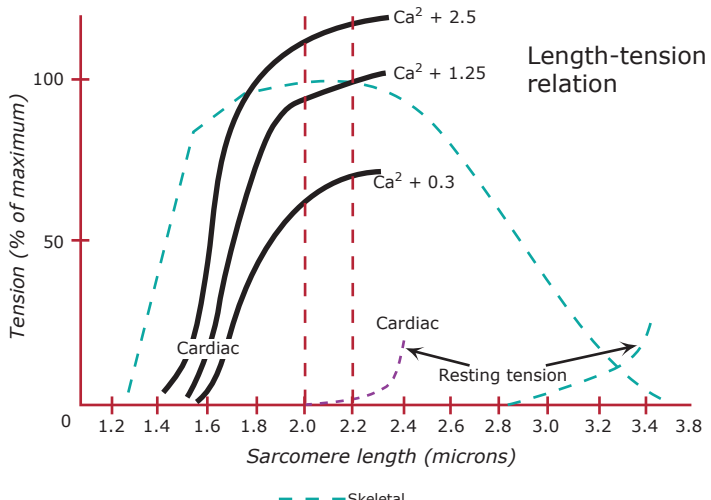


Figure by MIT OCW. After Opie, 1998.

The relationship between sarcomere lengths and tension for cardiac muscle in comparison with skeletal muscle. Note (i) the effect of increasing calcium ion concentration and (ii) the absence of any decrease of tension at maximal sarcomere lengths so that there is no basis for the descending limb of the Starling curve. Recent sophisticated laser-diffraction techniques invalidate previous curves based on apparent sarcomere length-tension relationships of imperfect papillary muscle preparations. For data on failing human heart, see Holubarsch et al. (1996). (From Opie 1998.)

Note that at sarcomere lengths greater than 3.65 microns developed tension is zero—presumably because there is no overlap between thick and thin filaments. The overlap increases as length decreases to 2.2 microns, and tension increases proportionately. As the sarcomere length decreases below 2.0 microns, developed tension decreases. The reasons are not clear, but may be related to changes in geometry, or level of “activation” of the contractile process.

Cardiac muscle exhibits a length-tension relationship which is not exactly the same as that for skeletal muscle. Figure 22 compares the length-tension curves for skeletal muscle and cardiac muscle. Both active and resting tensions are shown for isometric (constant length) contractions.

Resting tension is much greater in cardiac muscle than in skeletal muscle. In normal hearts, myocardial cells cannot be stretched much beyond the peak of the length-tension curve, and normally operate on the ascending limb of the curve.

Figure 23a,b shows length tension data obtained from cat papillary muscle. The scheme of the experimental apparatus is shown in Figure 23a. In its fully relaxed state the muscle exhibits the length-tension relationship shown in the “passive” curve of Figure 23b. It behaves as a non-linear spring. As the muscle reaches longer lengths it becomes increasingly stiff. The passive length-tension relationship is determined by the mechanical properties of the muscle cells and the associated connective tissue which is part of the muscle.

If the muscle contracts from a particular resting length and tension, it will develop *active* tension. Maximum tension will occur if the length of the muscle is fixed (*isometric contraction*). The active tension is a function of the initial resting tension (the preload). Higher developed tension is generated from longer resting lengths, and vice versa. The active tension curve in Figure 23b is a plot of active tension versus resting muscle length.

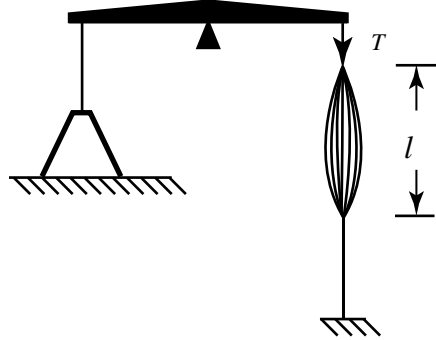
What happens if the muscle is allowed to shorten during the contraction phase? When the tension developed by the muscle reaches the afterload determined by the weight, the muscle will shorten until the final length-tension coordinates again fall on the active curve.

A first-order model for the papillary muscle might be a two-state spring as shown in Figure 23c. The spring constant K is low during the resting state, but is high during the active state of the muscle. The resultant length-tension curves would, of course, be linear, but they do capture the essence of the muscle's behavior as shown in Figure 23b.

2. Pressure-Volume Relationships in the Ventricle

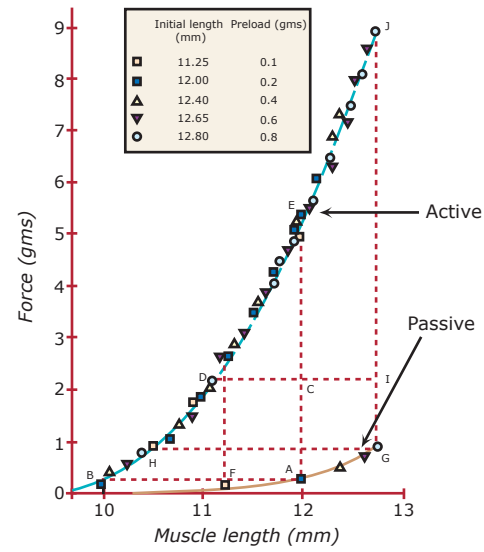
The intact heart exhibits mechanical behavior which resembles the length-tension behavior of isolated muscle. We will focus on a single ventricle. Instead of plotting tensions and lengths, it is much more convenient to measure and plot pressures and volumes. (One can relate intraventricular pressure to wall tension by appropriate application of LaPlace's law. Similarly, ventricular volume can be related to circumference.) A plot of ventricular pressure vs. volume is called a "ventricular function curve" and may be drawn for both the resting phase of the cardiac cycle (diastole) and the actively contracting phase (systole) (Figure 24). Such data may be obtained by filling the ventricle to different levels and measuring both diastolic pressure and volume to create the diastolic curve. Points on the systolic curve may be obtained by causing the ventricle to contract isovolumetrically (with the aorta clamped, for example) and measuring systolic pressure.

Figure 23
Isolated Cardiac Muscle Experiments



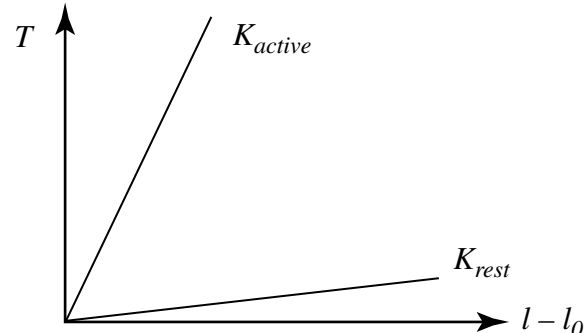
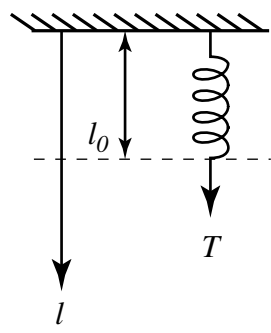
a. Experimental Apparatus

Relation Between Force (Tension) and Length for the Cat Papillary Muscle



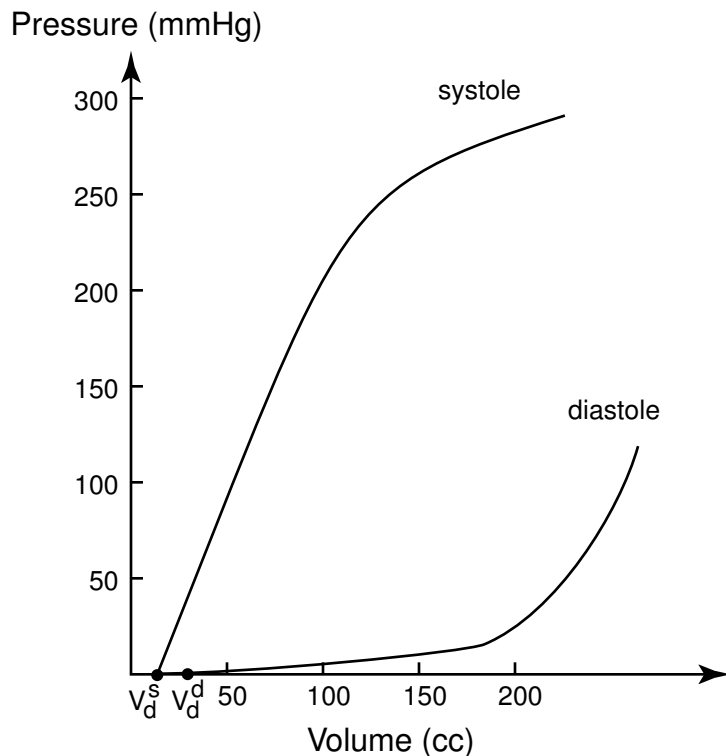
b.

Figure by MIT OCW. After Downing and Sonnenblick.



c. The Two-State Spring Model

Figure 24
Systolic and Diastolic Pressure-Volume Curves for the Left Ventricle



The systolic input-output relationship is sometimes referred to as the “Law of the Heart” or “Starling’s Law”. It has been shown in Figure 24 as a plot of maximum isovolumetric ventricular pressure vs. end-diastolic volume.

The “Law of the Heart” may be expressed in a variety of forms. Several “output” variables may be plotted on the ordinate including: ventricular pressure, stroke volume, cardiac output, stroke work, etc. A variety of “input” variables may be plotted on the abscissa including: end-diastolic volume, end-diastolic pressure, sarcomere length, circumference, etc. All of these variations may be seen in the literature, and they all express in some sense the input/output behavior of the ventricle as stated by Starling: “the energy of contraction is a function of the length of the muscle fiber”. This behavior of the heart is intrinsic to the myocardium itself, and is independent of any extrinsic neural or hormonal influences. One of the implications of Starling’s Law is that the “output of the heart is equal to and determined by the amount of blood flowing into the heart, and may be increased or diminished within very wide limits according to the inflow”...(Starling, 1918).

V_d is the volume of blood in the ventricle when the transmural pressure is zero. It is referred to as the “dead volume” or “zero-pressure filling volume”. V_d is generally *not* the same

during diastole and systole, as is indicated in Figure 24. Estimates of the dead volumes during systole and diastole are given below in Table 5 (page 44).

If as shown in Figure 25 an isolated left ventricle is filled with a constant *preload* pressure, P_f , and if the aorta is connected to a constant *afterload* pressure, P_a , a pressure-volume loop will be generated during the heart's pumping cycle, as shown in Figure 26. The cycle begins at (1) when the heart is at end-diastolic pressure and volume, P_f . From 1 to 2 the ventricle contracts with no change in volume (*isovolumetric contraction phase*) since both mitral and aortic valves are closed. From 2 to 3 the ventricular volume decreases as blood is ejected into the afterload reservoir at constant pressure, P_a . Ejection continues until the systolic pressure-volume curve is reached at point 3. From 3 to 4 the pressure drops during the *isovolumetric relaxation phase* when aortic and mitral valves are closed. At point 4 the mitral valve opens and filling takes place at constant pressure, P_f , until the volume again reaches point 1 on the diastolic pressure-volume curve.

Figure 25
Cardiac cycle with constant preload, P_f , and constant afterload, P_a

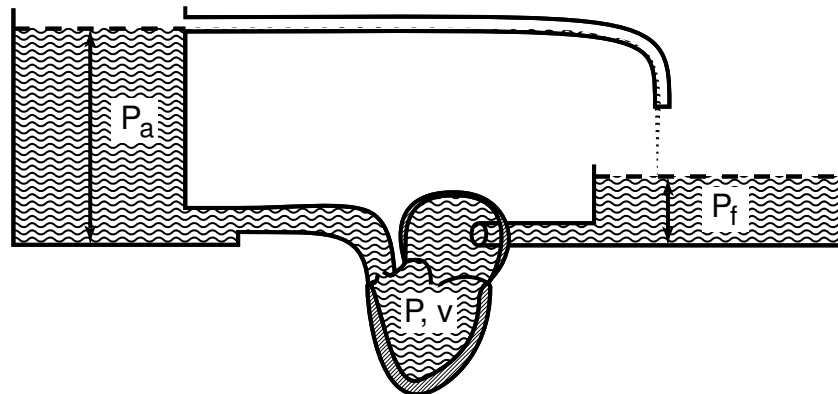


Figure 26
Pressure-volume loop during constant pre- and afterload

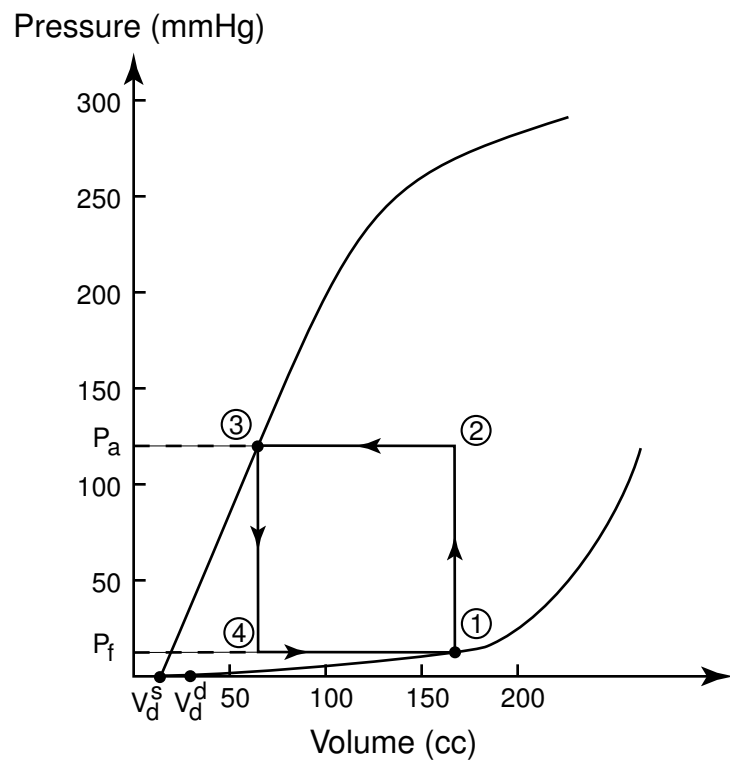


Figure 27
Left ventricular (LV), aortic, and left atrial (LA) pressure versus time

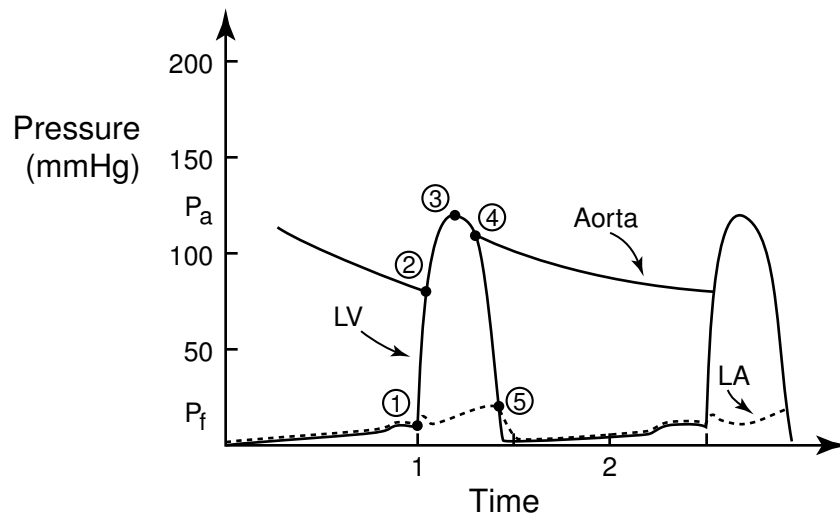
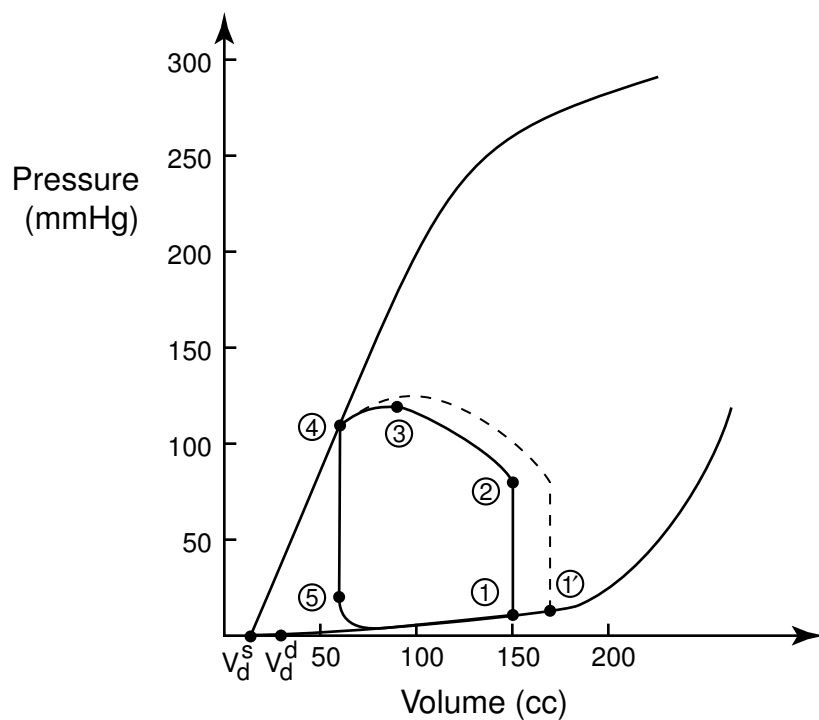


Figure 28
The LV pressure-volume loop when the heart is attached to the aorta



If the heart functions within the intact circulation the LV preload is determined by the left atrial pressure, and the afterload is determined by the pressure in the aorta. Figure 27 shows the pressures in LA, LV, and aorta as a function of time. The corresponding LV pressure-volume loop is shown as 1-2-3-4-5 in Figure 28. (These key pressure-volume points are also indicated in Figure 27.)

During diastole, the ventricle fills from point (5) to point (1) along its diastolic curve. The **end-diastolic** pressure at point (1) is the *preload*. Systole begins, and the ventricle begins to contract, thus increasing its pressure, but since both mitral and aortic valves remain closed, the ventricular volume remains constant (isovolumetric contraction). At point (2), the intraventricular pressure exceeds aortic pressure and ejection begins. The pressure at point (2) is the *afterload*.¹ The maximum pressure is reached at point (3), and is called “systolic BP” when measured in arteries.

At the end of systole, point (4), the ventricular volume and pressure are defined by the systolic ventricular function curve. Diastole then begins, with isovolumetric relaxation of the ventricle to point (5) where filling begins again. Notice that the same amount of blood is pumped out of the heart during systole as enters during diastole. If diastolic flow into the heart increases (assume an end-diastolic volume of 170 ml), then the end-diastolic operating point would be at (1)'—an increased preload. If systolic ejection occurs at the same afterload, all of this blood is ejected and the end-systolic point is again at (4). Since the stroke volume has increased, the work performed by the heart during the new cycle has also increased. Note that stroke work, $\int pdV$, is simply the area enclosed by the P-V loop.

3. Contractility

In the intact organism Starling’s law of the heart probably plays a rather *minor* role in changing cardiac output to meet the varying needs of the body. The law’s major value is probably in balancing the outputs of the right and left ventricles on a beat-by-beat basis.

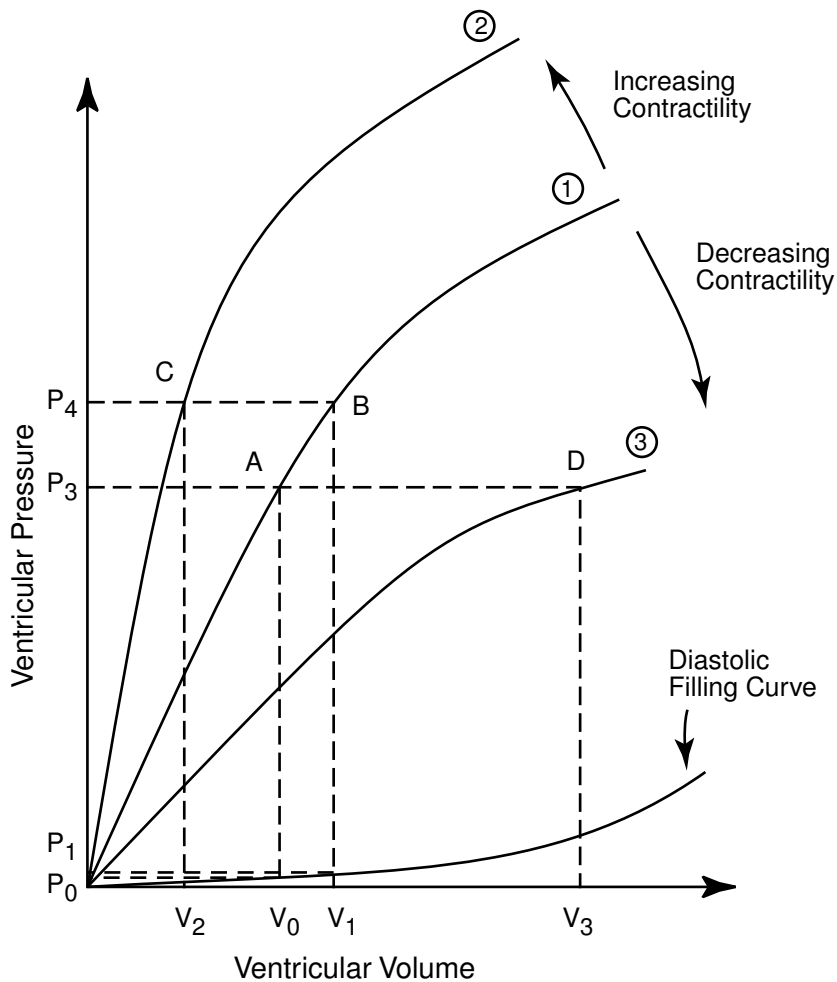
How, then, does the body increase cardiac output to meet increased metabolic needs, as during exercise, for example? Cardiac output increases dramatically, but the ventricular filling pressure and volume typically show *no* increases. Rather, the ventricular pressure-volume relationship actually changes so that for the same filling volume, a greater pressure is developed. (See Figure 29.) The heart becomes a more powerful or more “contractile” pump. Changes in

¹It is probably more precise to consider wall tensile stress (tension per unit cross sectional area) as the afterload rather than ventricular pressure. The same ventricular pressure would lead to a greater afterload if the radius of the heart were larger, and vice versa. If we consider wall thickness as well, then hypertrophy may actually reduce the afterload of individual fibers.

cardiac contractility are mediated by physiologic signals extrinsic to the heart that are carried by the autonomic nervous system, hormones, or by drugs. Contractility changes may also be caused by disease.

Figure 29 illustrates how changes in contractility result in shifts of the ventricular end-systolic function curve.

Figure 29



A shift in the curve upward and to the left represents an increase in contractility and vice versa. Notice that we may cause an increase in isovolumetric end systolic pressure by moving along curve 1 from A to B. This corresponds, of course, to increasing the preload from P_0 to P_1 , and involves no change in cardiac contractility. If, by virtue of an extrinsic influence on the heart, ventricular contractility increases (curve 2), the same increase in systolic pressure may be achieved at a *net decrease* in filling pressure (point C). In general, changes in contractility occur in the intact animal to meet changes in demands. Extrinsic influences may also decrease contractility (curve 3).

In this case, a large increase in preload would be required just to maintain the same end systolic pressure (point D). Disease and certain drugs may cause such decreases in contractility. Any agent causing an increase in contractility is called a **positive inotropic agent** and vice versa.

The diastolic pressure-volume curve is a measure of the mechanical stiffness of the heart during its resting phase. The *relaxation* of muscle follows the active removal of calcium ions from the region of the contractile apparatus by the sarcoplasmic reticulum. Thus, it is an energy-requiring process. The diastolic properties of the heart may be significantly affected by a variety of pathologic conditions which alter the mechanical properties of the ventricle either through changes in *structure* (constrictive pericardial disease, cardiac tamponade, dilated cardiomyopathy, etc.) or *function* (ischemia, hypertrophic cardiomyopathy). For example, Figure 30 illustrates the increase in diastolic stiffness associated with transient lack of blood flow to the heart due to coronary artery disease. The increase in diastolic stiffness reflects a relative lack of ATP that is required for muscle relaxation.

Figure 30

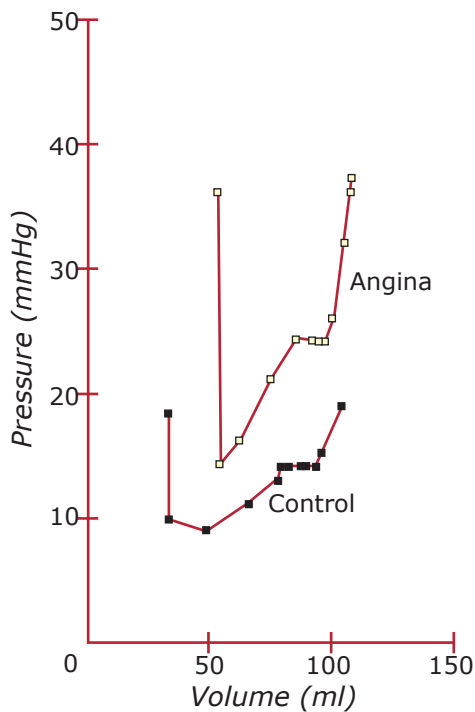


Figure by MIT OCW. After Grossman and Barry, 1980.

Left ventricular diastolic pressure-volume plots in control (open circles) and post-pacing (closed circles) periods in a patient with coronary heart disease who developed angina during atrial pacing. The entire diastolic pressure-volume relationship is shifted upward, so that pressure is higher at any given volume. (From Grossman and Barry 1980.)

B. Model of the Heart

In this section we wish to develop a simple model of the heart which will be intuitively reasonable, which will account for the input/output relationships of the heart on both a time-averaged basis and a beat-by-beat pulsatile basis. The model must also reflect the concept of “contractility”. Our model is based on the work of Defares (Defares, Osborn, and Hara 1963), which was subsequently elaborated by Prof. Kiichi Sagawa and his colleagues at Johns Hopkins. Sagawa has written an excellent review of ventricular models (Sagawa 1973), including that of Defares.

1. The Variable Capacitor Model

Before going to the modeling, an examination of some experimental data is necessary. Figure 25 shows a series of pressure-volume loops from a denervated canine left ventricle obtained under different conditions of preload and afterload, but during a constant contractile state.

Figure 31

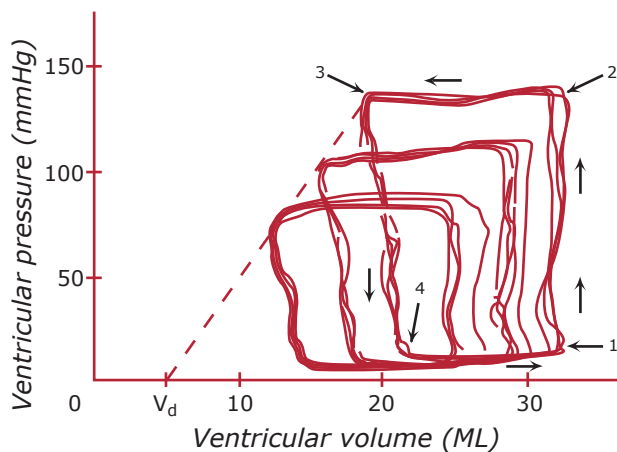


Figure by MIT OCW. After Suga and Sagawa 1972.

Notice that during diastole, there is an approximate straight-line relationship between pressure and volume. At zero pressure the line crosses the volume axis at V_d , the residual (or “dead”) volume of the ventricle when the transmural pressure is zero. Note also from Figure 31

that the end-systolic points fall on a straight line which has the same volume intercept,² but a much larger slope.

This experimental data suggests that we may consider the left ventricle as a 2-state device. In diastole it behaves as an elastic chamber (a capacitor) whose properties may be represented by the diastolic pressure-volume curve shown in Figure 26. In the physiologic range, the curve is a straight line, and its equation would be:

$$V = V_d + C_D P \quad (30)$$

Note that $C_D = \Delta V / \Delta P$, and is termed the *diastolic capacitance* (or compliance) of the ventricle. Similarly, during systole the heart may be represented as a capacitor with value, C_S . The pressure volume relation would be:

$$V = V_d + C_S P \quad (31)$$

This relation is plotted as the systolic curve of Figure 32. Notice that at high diastolic filling pressures the diastolic pressure-volume curve is no longer linear. This occurs, however, at diastolic filling pressures greater than about 20mmHg, which is above the normal physiologic range, and where cardiac dilatation begins to be limited by collagenous tissue and pericardium. Approximate values of the capacitances and dead volume for dog and man are shown in Table 5.

²Note: for simplicity we will assume that the dead volume, V_d , is identical for diastole and for systole.

Figure 32
Schematic Ventricular Pressure-Volume Relations

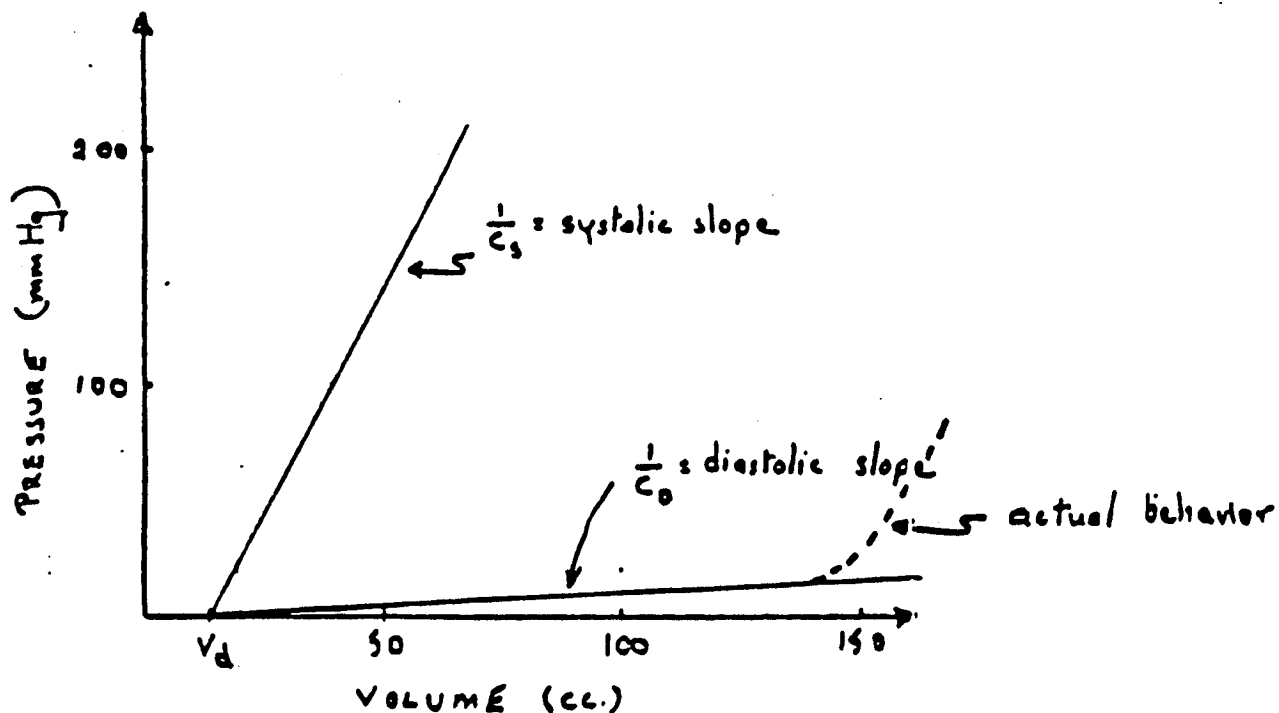


Table 5
Approximate Values for Capacitances and V_d s for Dog and Man

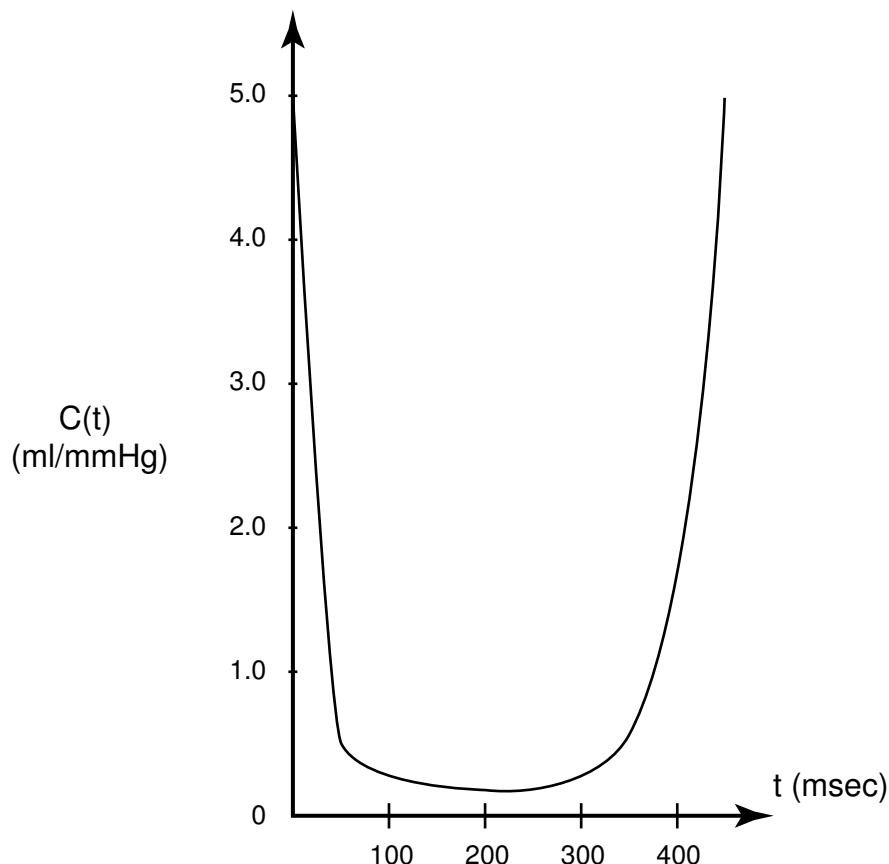
	Dog	Man
V_d	5 cc	15 cc
C_D	4 ml/mmHg	15 ml/mmHg
C_S	0.1 ml/mmHg	0.4 ml/mmHg

So far we have considered the ventricle to be a discrete two-state device with instantaneous transitions from diastole to systole and back. In reality, of course, the properties of the ventricle change continuously, and ventricular capacitance is a continuous function of time $C(t)$, where

$$C(t) = \frac{V(t) - V_d}{P(t)} \quad (32)$$

This function has been experimentally measured in dogs by Suga and Sagawa (1975). By measuring instantaneous pressure-volume relationships during systole, the function $C(t)$ was calculated, and the result is shown in Figure 33.

Figure 33
Instantaneous LV Capacitance, $C(t)$ for the dog



Curve calculated from data in Suga (1979).

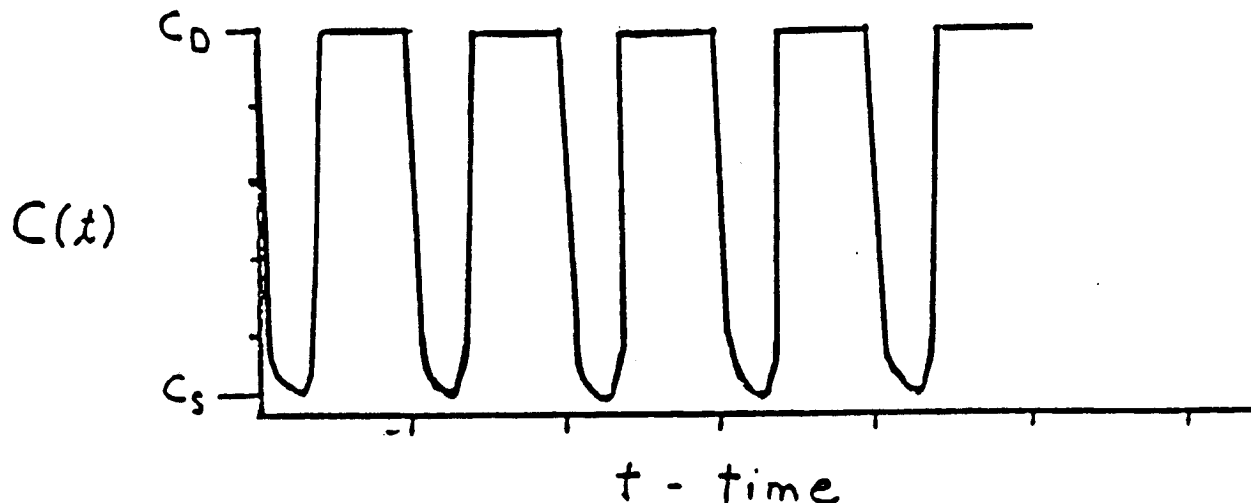
Notice that in this experiment $C(t)$ decreases from its diastolic value over a 270 ms period, then relaxes back to its diastolic value during the ensuing 135 ms period. The time to develop minimal capacitance is approximately twice the relaxation period.

The instantaneous capacitance $C(t)$ is independent of preload and afterload and provides a complete quantitative description of the mechanical properties of the ventricle during the cardiac cycle.

We will now proceed to analyze how we may utilize the instantaneous capacitance to calculate the variables such as stroke volume and cardiac output.

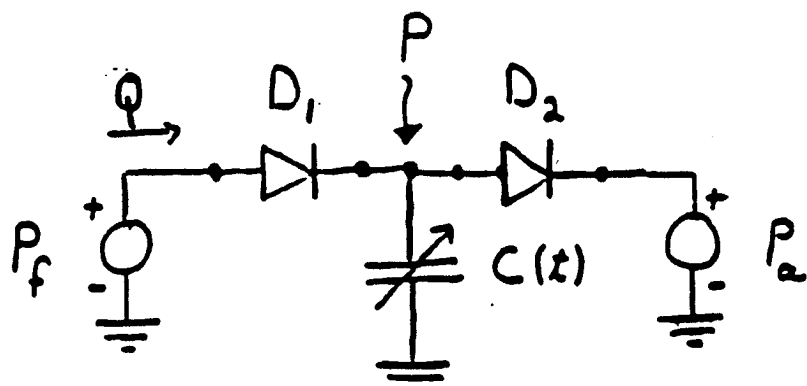
In Figure 34 we plot $C(t)$ for a number of cardiac cycles.

Figure 34



We next analyze the pump function of the idealized LV when it is driven by a constant pressure preload P_f , and when it pumps into a constant pressure afterload, P_a . To do so, consider the following electric circuit model of the system.

Figure 35
Electrical Circuit Model of the Ventricle



Here the open circles represent constant pressure sources. D_1 is a diode representing the atrio-ventricular valve; D_2 is a diode representing the ventricular outflow valve. (A diode may be in two states: conducting and non-conducting. In the conducting state, the resistance is zero and current may flow, and vice-versa.) “Ground” represents the pressure outside the ventricle which

would be atmospheric pressure in the case of an isolated left ventricle or an open-chest experiment. The variable capacitor represents the LV.

Pressure across the capacitor is given by

$$P(t) = \frac{V(t) - V_d}{C(t)} \quad (33)$$

We now analyze the system during each phase of the cardiac cycle:

- 1) **Isovolumic Contraction.** During the period of diastolic filling, the capacitor has filled to a level:

$$V_D = C_D P_f + V_d$$

Now as $C(t)$ decreases below its diastolic value of C_D , $P(t)$ will increase above P_f , and D_1 stops conducting. The Diode D_2 is still non-conducting since $P(t) < P_a$. Therefore, no flow occurs and $V(t) = V_D$. The capacitance decreases until

$$C(t) = \frac{V_D - V_d}{P_a} = \frac{C_D P_f}{P_a}$$

At this point, $P(t) = P_a$, D_2 conducts and the ejection phase begins.

- 2) **Ejection Phase** - D_1 remains non-conducting since $P(t) > P_f$. D_2 is conducting, and $P(t) = P_a$. The volume in the capacitor at the end of systole is given by

$$V_S = C_S P_a + V_d$$

- 3) **Isovolumic Relaxation** - As soon as $C(t)$ increases above its minimum value of C_S , $P(t)$ drops below P_a , and D_2 stops conducting. D_1 will also remain non-conducting until $P(t)$ drops to P_f . This occurs when

$$C(t) = \frac{V_S - V_d}{P_f} = \frac{C_S P_a}{P_f}$$

4) **Diastole** - During diastole the outlet diode D_2 remains non-conducting since $P_a > P(t)$. The inlet diode D_1 conducts and the capacitor charges with $P(t) = P_f$. The end diastolic volume V_D becomes

$$V_D = C_D P_f + V_d$$

Phases 1 and 2 are usually considered part of ventricular systole; phases 3 and 4 are usually considered part of ventricular diastole. Figure 36 presents a sketch of the functions $C(t)$, $P(t)$ and $V(t)$, while Figure 37 plots the resultant pressure-volume loop.

Figure 36
Sketch of $C(t)$, $P(t)$ and $V(t)$

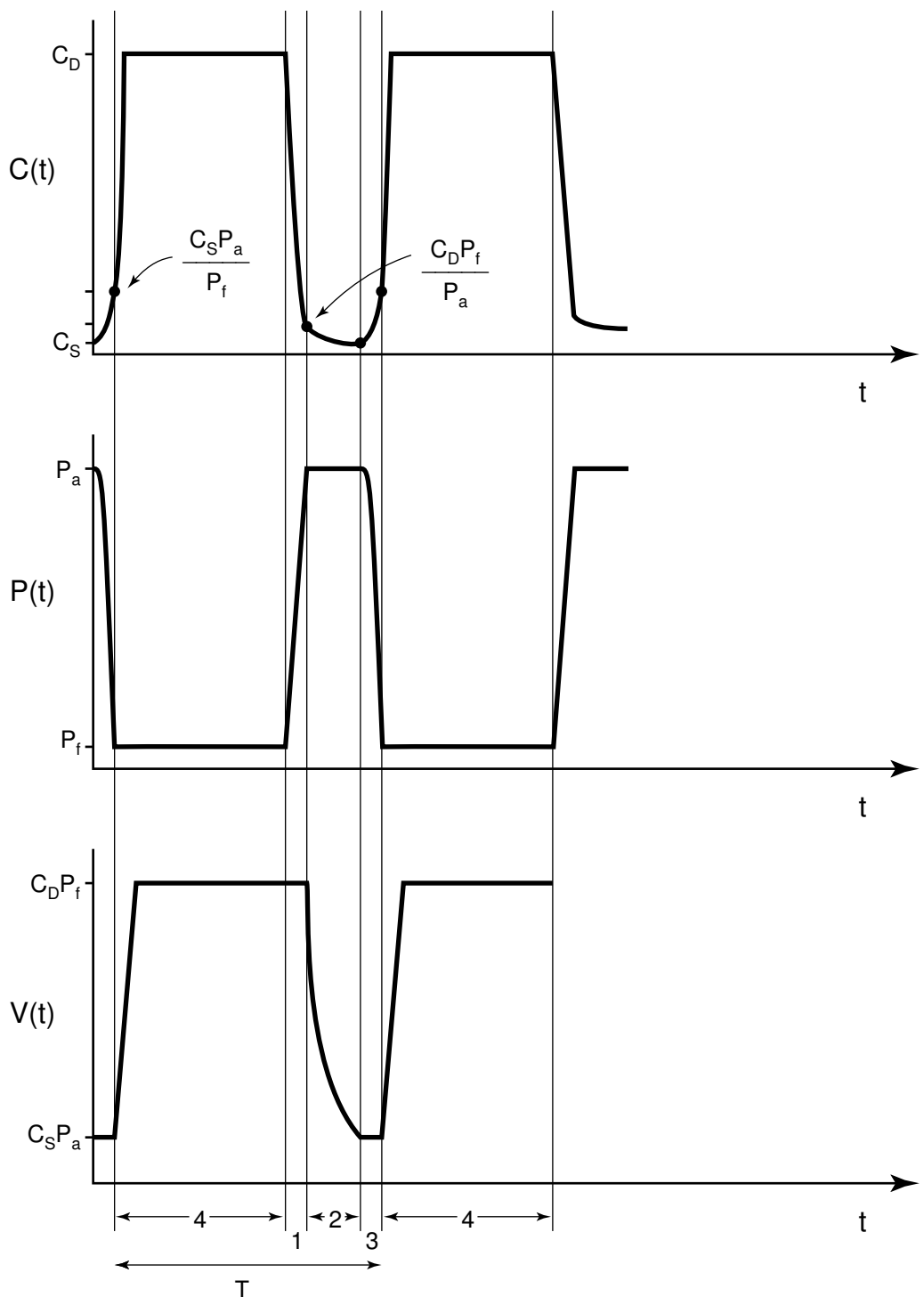
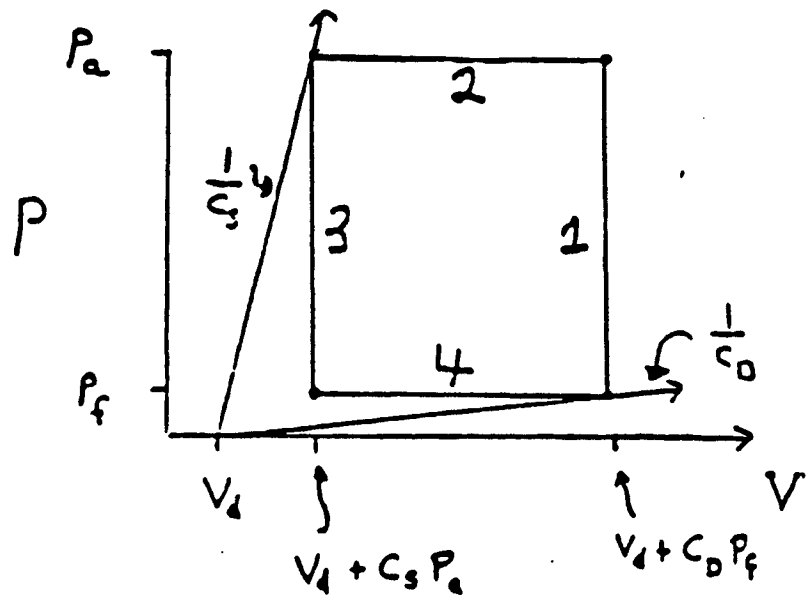


Figure 37
Cardiac Cycle in the Pressure-Volume Plane



The stroke volume of the ventricle is given by the difference between its end-diastolic and end-systolic volume.

$$S.V. = V_D - V_S$$

$$S.V. = C_D P_f - C_S P_a \quad (34)$$

The ventricular output, V.O., is given by the heart rate, f, times the stroke volume.

$$V.O. = f \times S.V.$$

$$V.O. = f(C_D P_f - C_S P_a) \quad (35)$$

where f is given by

$$f = 1/T$$

and T is the length of one cardiac cycle.

These equations for stroke volume and ventricular output were derived for constant pressure preload and afterload. Actually, they are valid for arbitrary preload and afterload if P_f and P_a represent the end-diastolic and end-systolic (i.e. end-ejection) pressures, and as before C_D and C_S

represent the end-diastolic and end-systolic capacitances. In particular, one must be aware that P_a may differ substantially from the mean arterial pressure.

Note that if $P_f < P_a C_S / C_D$, no ventricular output results. When P_f is large, we find experimentally that the ventricular output curve flattens out (see Figure 38). This occurs because the diastolic pressure-volume curve is not linear for large values of P_f . (See Figures 32, 39.) A reasonable (piecewise linear) modified model for the diastolic filling curve is therefore:

$$V = V_d + C_D P_f \quad \text{for } P_f < \frac{V_{\max}}{C_D}$$

$$V = V_d + V_{\max} \quad \text{for } P_f > \frac{V_{\max}}{C_D}$$

Ventricular output is then given by:

$$\begin{aligned} V.O. &= f(C_D P_f - C_S P_a) && \text{if } \frac{P_a C_S}{C_D} < P_f \leq \frac{V_{\max}}{C_D} \\ &= f(V_{\max} - C_S P_a) && \text{if } P_f \geq \frac{V_{\max}}{C_D} \\ &= 0 && \text{if } P_f < \frac{P_a C_S}{C_D} \end{aligned} \tag{36}$$

Figure 38
Ventricular Output as a Function of LV Filling Pressure, P_f

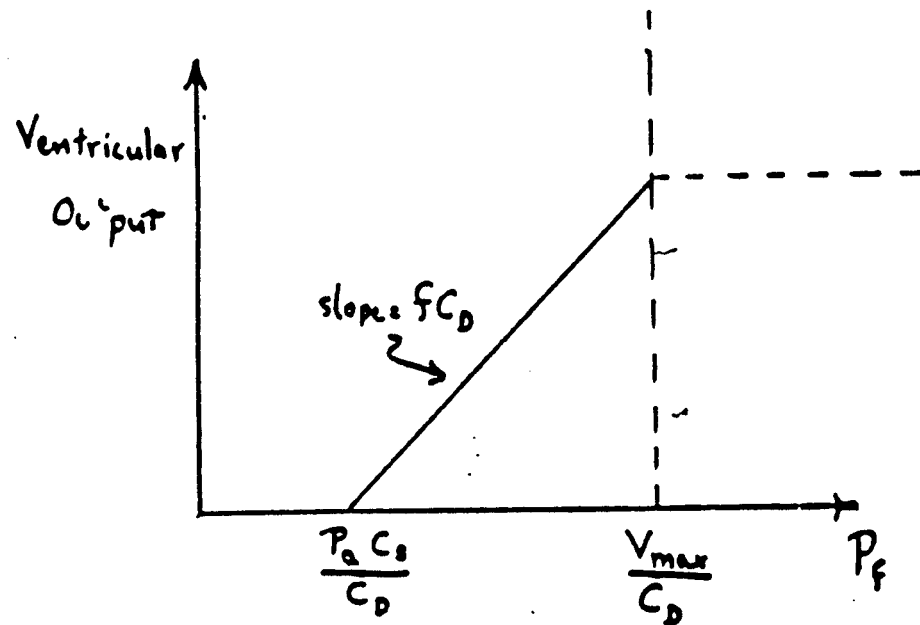
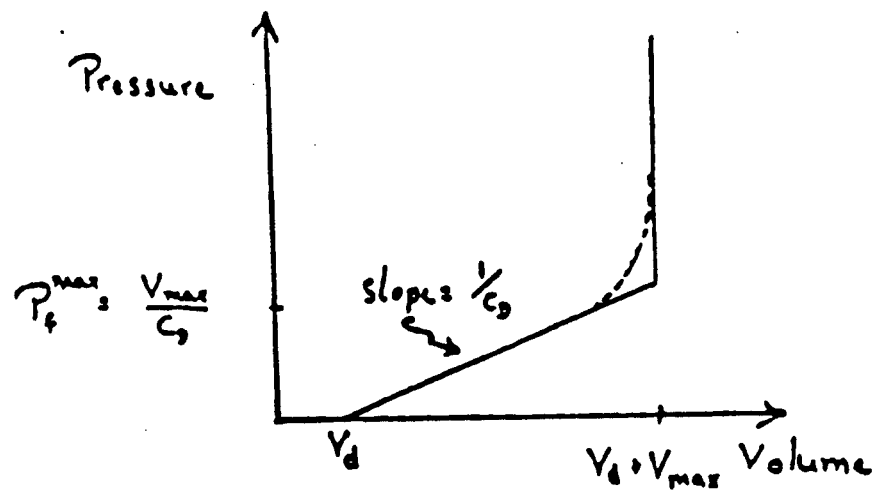


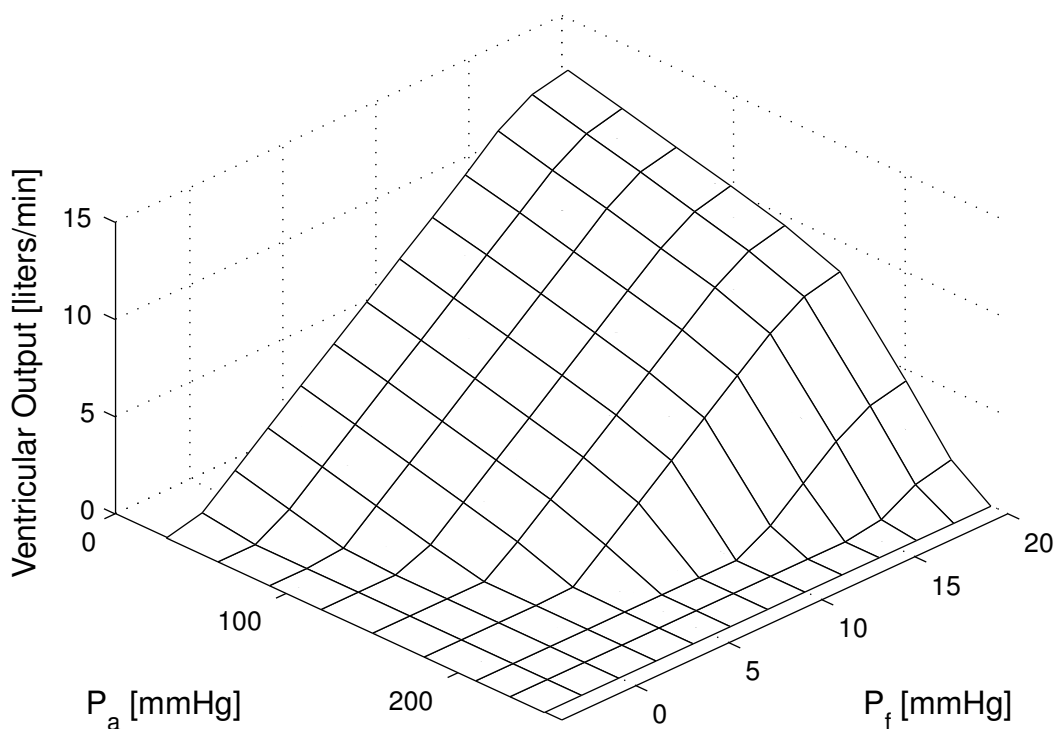
Figure 39
Diastolic Filling Curve



Equation 36 relates ventricular output to filling pressure, P_f . It is plotted in Figure 38. This plot will be referred to as a **ventricular function curve**. Since ventricular output depends on afterload, P_a , as well as preload, a 3-dimensional surface is required to fully characterize ventricular function. Such a plot is shown in Figure 40, using data produced by a computational model of the

cardiovascular system (courtesy of Dr. Ramakrishna Mukkamala, 2000). Notice that for the single ventricle pump, output is quite sensitive to both preload and afterload.

Figure 40
Ventricular Output as a Function of Preload and Afterload
(Data produced by a computational model of the cardiovascular system)



The variable capacitor model also permits us to calculate the maximum pressure developed by the left ventricle when aortic outflow is occluded. Such *isometric contractions* have proven to be useful experimental techniques in studying cardiac contractility.

If we set stroke volume to zero in equation (34) we find:

$$S.V. = 0 = C_D P_f - C_S P_a$$

$$\begin{aligned} P_a^{\max} &= \frac{C_D P_f}{C_S} && \text{if } P_f < \frac{V_{\max}}{C_D} \\ P_a^{\max} &= \frac{V_{\max}}{C_S} && \text{if } P_f > \frac{V_{\max}}{C_D} \end{aligned} \quad (37)$$

Experimental data from isovolumetric contractions in the dog heart during constant inotropic state are shown in Figure 41. Again note the reasonableness of the straight-line approximations, and the fact that for this particular preparation the ratio of C_S/C_D is approximately one tenth.

Figure 41
Isovolumetric Contraction

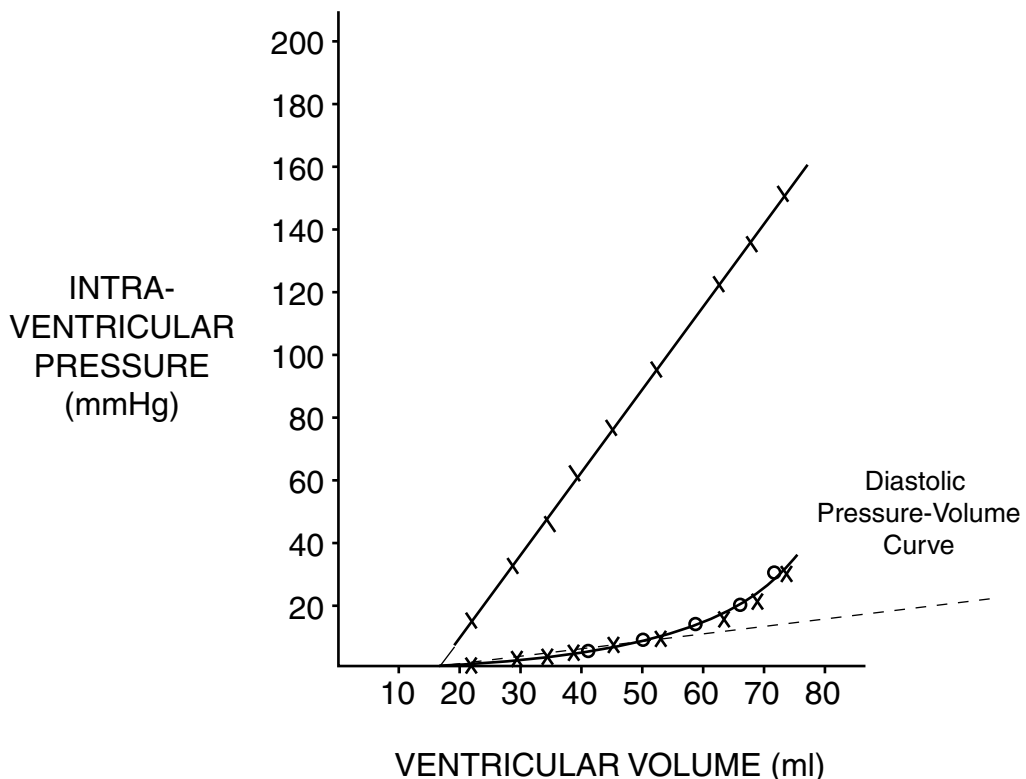


Figure 42 illustrates a series of beat-by-beat left ventricular pressure-volume loops measured in humans using an *impedance catheter* to estimate ventricular volume (McKay et al. 1984). Transient vena cava obstruction was used to vary the preload. Notice the approximately linear relationship between end systolic pressure and relative volume.

Figure 42
Pressure Volume Loops from Humans Using an Impedance Catheter

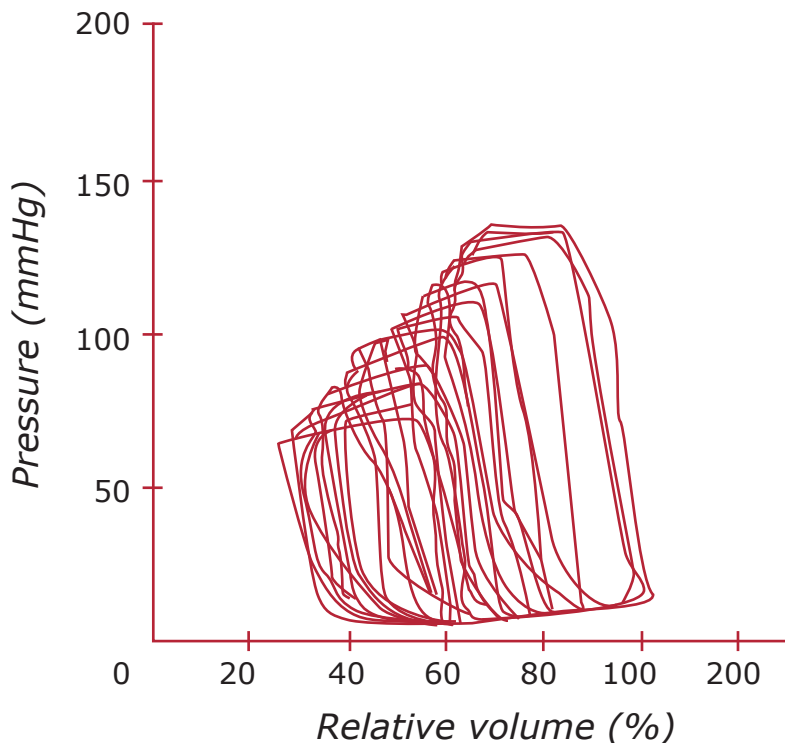
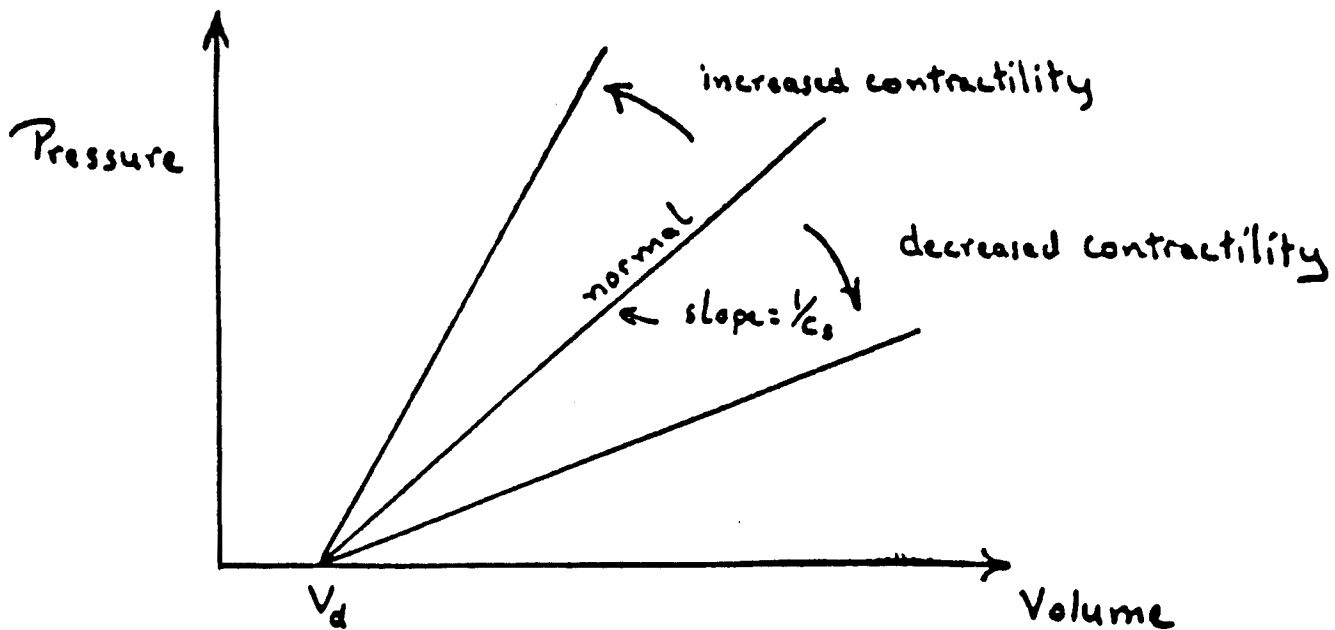


Figure by MIT OCW. After McKay et al. 1984.

2. Inotropic State (“Contractility”)

The value of the systolic capacitance, C_S , determines the “inotropic” or “contractile” state in our model: the smaller C_S the more contractile the heart, and the steeper the slope of the systolic P-V curve (Figure 43). (Can you predict the change to be expected in the pressure-volume loop as the contractility increases while keeping the preload and afterload constant?)

Figure 43
Representation of Contractility in the P-V Plane



Positive inotropic drugs result in a decrease in C_S while generally leaving C_D unaffected. Figures 44 and 45 present experimental data showing that the positive inotropic action of epinephrine infusion leads to a clear increase in systolic “elastance, $e(t)$ ”. Elastance is the inverse of compliance [$e(t) = 1/C(t)$]. Figure 44 shows that measurements of ventricular volume or pressure alone cannot satisfactorily characterize ventricular contractility. At a fixed inotropic state, for example, there may be wide variations in stroke volumes and developed pressures. On the other hand, plots of elastance ($\Delta P/\Delta V$) vs time reveal consistent changes with inotropic state. The pressure-volume loops of figure 45 also demonstrate the unique value in using end-diastolic pressure-volume ratios as a measure of contractile state.

Figure 44

Image removed due to copyright considerations. See Figure 4 in Sunagawa, K. and Sagawa, K. 1982. Models of ventricular contraction based on time-varying elastance. *CRC Critical Reviews in Biomedical Engineering*, vol. 7, issue 3.

Figure 45

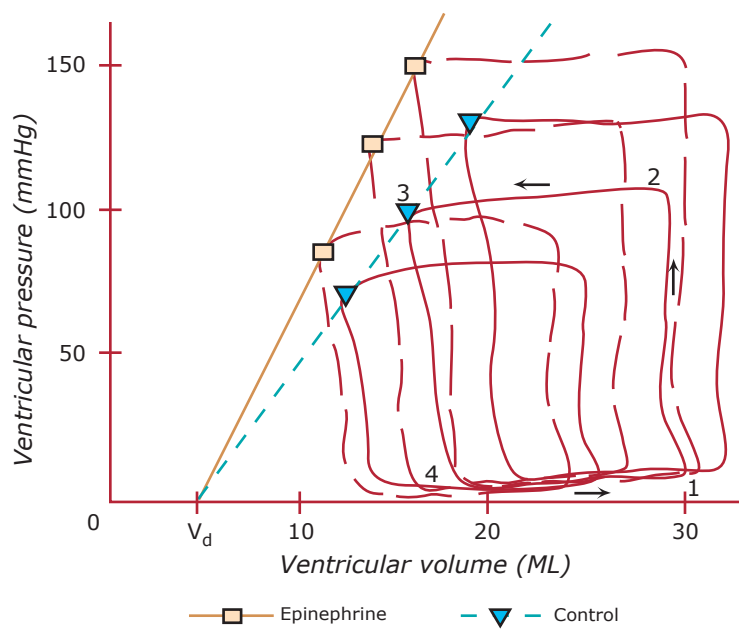


Figure by MIT OCW. After Fig. 5 in Sunagawa and Sagawa, 1982, based on experiments by Suga, Sagawa and Shoukas, 1973.

Figure 46 shows ventricular function curves from an isometrically contracting dog heart with various interventions. Notice that the positive inotropic drugs lanatoside C and epinephrine both increase the slope of the systolic P-V curve, but do not change the diastolic curve.

Figure 46
Ventricular Function Curves Showing Effect of Several Inotropic Drugs

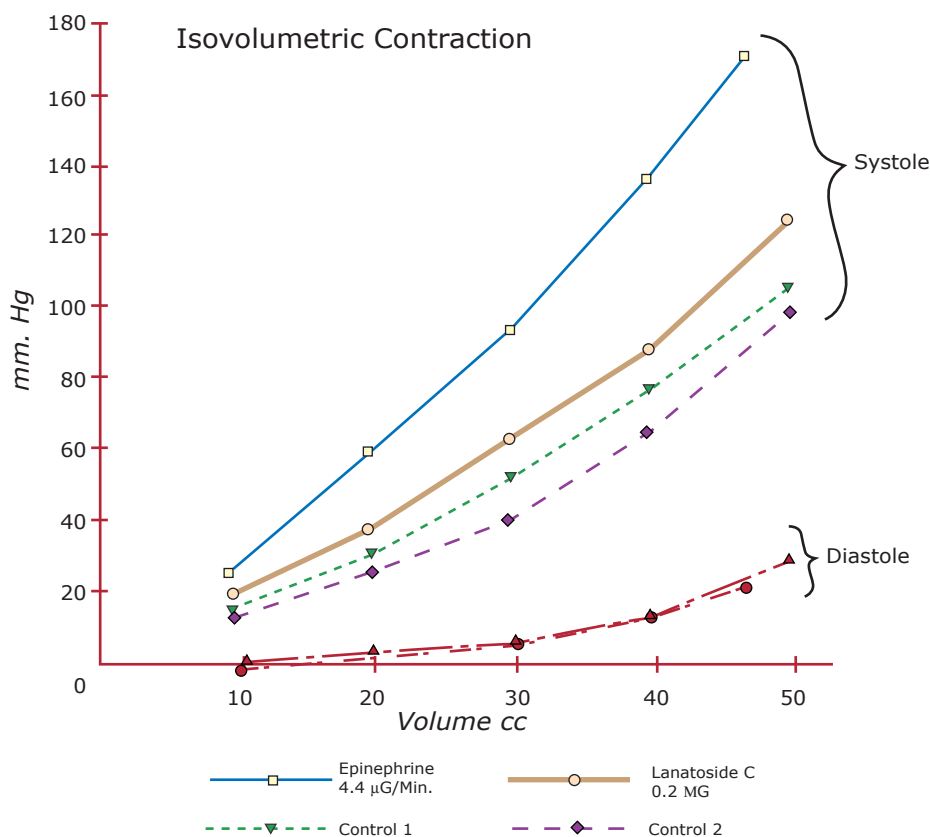


Figure by MIT OCW.

Measurement of end-systolic capacitance in the clinical setting is now becoming an accepted standard, but presents significant practical difficulties. One must obtain simultaneous measures of both ventricular pressure and ventricular volume. In addition, these measurements must be made at a variety of filling volumes in order to define the linear relation between end systolic pressures and volumes which determines C_s .

Several techniques have been used to achieve the required measurements. One approach monitors ventricular pressure via a catheter-tipped transducer and determines ventricular volumes using radionuclides. Ventricular filling volumes are varied by manipulating pre-load (nitrites) and afterload (nitroprusside, or α -adrenergic drugs).

A second technique makes use of the “impedance catheter”. A single catheter measures LV pressures, and also estimates LV volume by monitoring the electrical impedance of the blood-filled chamber. The resulting data may be plotted as P-V loops. The technique is useful in documenting relative changes in ventricular contractility induced by therapeutic maneuvers, for example. Figure 47 shows the positive inotropic effect of dobutamine, and Figure 48 shows a similar effect of epinephrine. (In each figure, the control loops show the lower end-systolic P-V slope.) A balloon in the inferior vena cava was transiently inflated to rapidly vary the ventricular filling volumes in these experiments.

Figure 47
Pressure-Volume Loops in Man Using an Impedance Catheter.
a) Control, b) Dobutamine

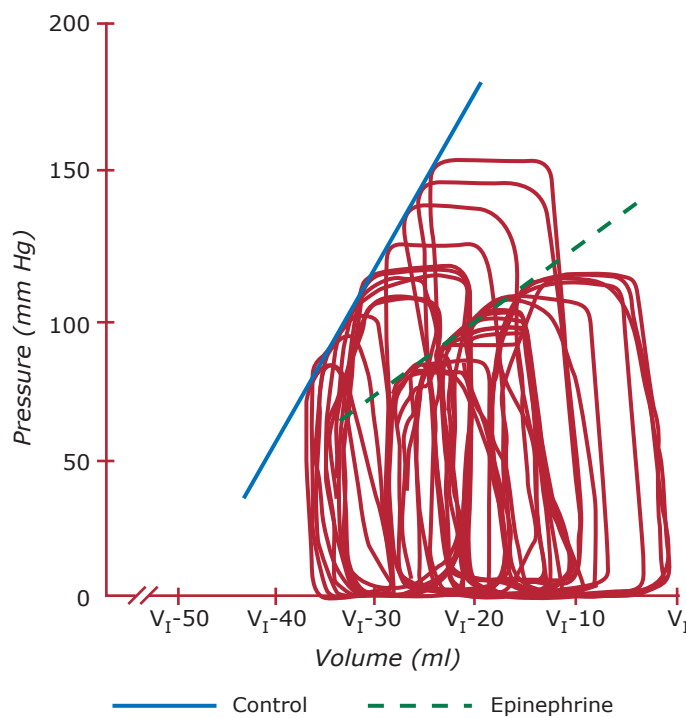


Figure by MIT OCW.

Figure 48
Pressure-Volume Loops in Man Using an Impedance Catheter
a) Control, b) Epinephrine

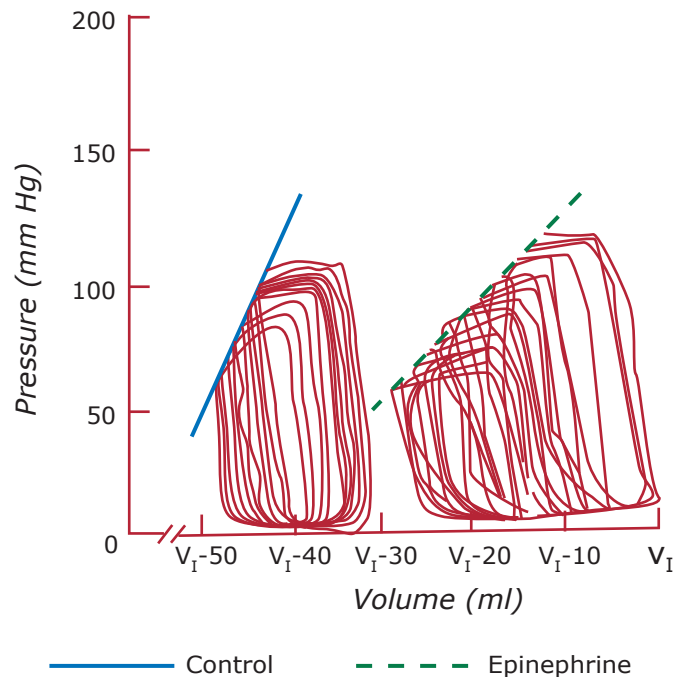


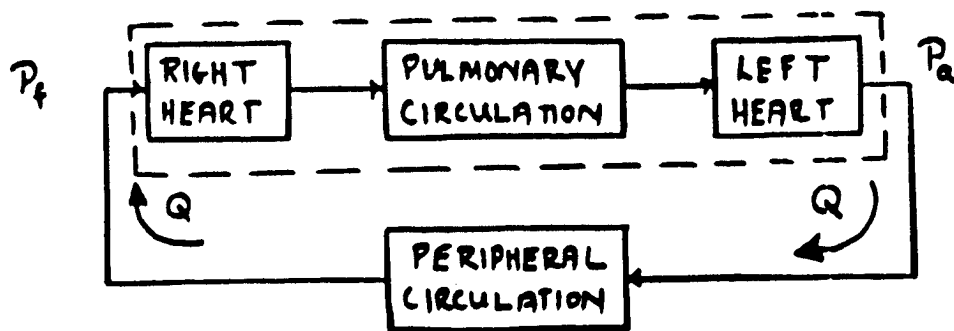
Figure by MIT OCW.

C. Heart-Lung Pumping Unit

1. “Open Chest” Model

The complete circulation consists of two pumps arranged in series with two vascular beds as shown in Figure 49. Each pump is modeled as a single variable capacitor.

Figure 49
Diagram of the major elements of the circulatory system.
The elements enclosed in the dotted rectangle are included in the “heart-lung pumping unit”.



This simple approach ignores the atria completely, and combines the effect of the atrial kick³ into a single pumping chamber. There is good experimental data to confirm the validity of using the variable capacitor model for the right heart as well as the left (Sunagawa and Sagawa 1982).

The pulmonary vascular bed is modeled in the same manner as the systemic bed, although the properties of the pulmonary vascular resistance differ (see below).

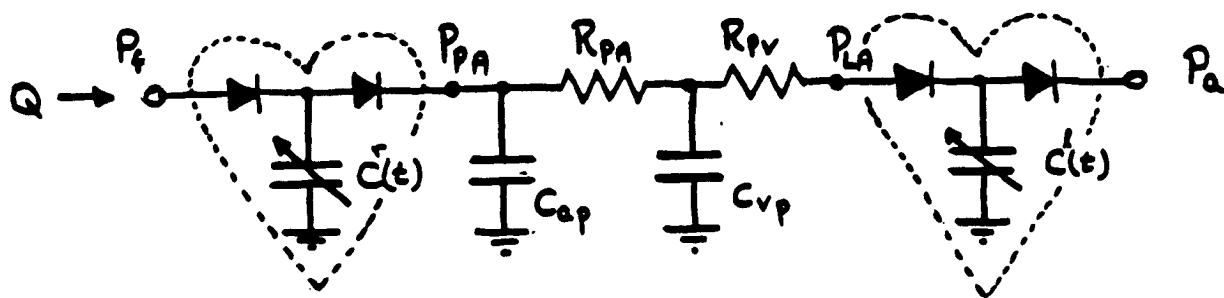
It is often convenient to combine the heart (both right and left chambers) together with the pulmonary circulation as a single functional unit. This so-called “**heart-lung pumping unit**” would be described in terms of a “cardiac” output, Q , and a venous filling pressure, P_f . The interaction of the heart-lung pumping unit with the systemic circulation is of fundamental interest clinically.

How can we characterize the heart-lung unit? It is sketched in Figure 50. The preload to the heart-lung unit (HLU) is the right atrial filling pressure, P_f , and the afterload is the aortic pressure, P_a . A rigorous derivation of the properties of the HLU would require a detailed analysis

³Atrial contraction does contribute to the efficiency of the heart by increasing the ventricular end-diastolic pressure. The atrial “kick” may increase cardiac output by 15-20% under certain conditions of severe cardiac demand.

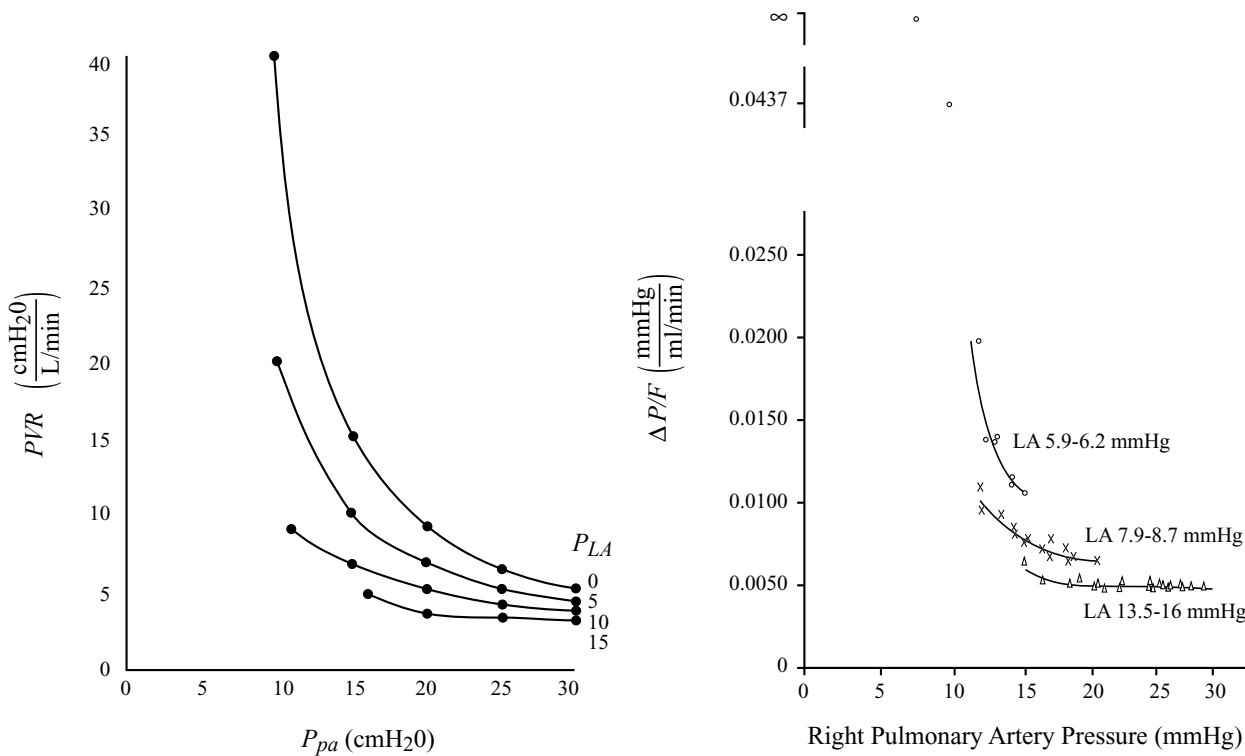
of the pulmonary circulation. A simplified and somewhat qualitative approach will be developed here.

Figure 50
The Heart-Lung Pumping Unit



The right ventricle and pulmonary circuit are a low-pressure system. Normal mean pulmonary artery pressure, P_{PA} , is approximately 15 mmHg. The pulmonary vascular bed changes its resistance significantly as a function of flow rate. As the pulmonary artery flow increases (as a result of somewhat higher driving pressures), its resistance *decreases*. The reason for this behavior is probably that multiple possible parallel pathways for blood flow exist in the pulmonary bed. As flow increases, more parallel branches are recruited, thus lowering resistance. In addition, the vessels dilate with increasing transmural pressure, also decreasing resistance to flow. Recruitment and dilation of vessels also occurs as the left atrial pressure increases. Permutt (see Sagawa 1973, p. 46) suggested a model for the pulmonary vascular bed which consisted of a parallel array of thin-walled collapsible tubes (Starling resistors). Alveolar pressure was the pressure external to the collapsible segments. This model predicted a relationship between pulmonary vascular resistance and pulmonary arterial pressure which was highly non-linear. (See Figure 51a.) Experimental data (Figure 51b) seem to confirm this model.

Figure 51



A. Relationship between pulmonary vascular resistance, PVR (ordinate), and pulmonary arterial pressure P_{pa} (abscissa) under four different left atrial pressures, P_{LA} , and a single alveolar pressure P_{alv} . $H_T = 20 \text{ cm}$; $R_T = 2.5 \text{ cm H}_2\text{O/liter per minute}$. Computed from Permutt's model of pulmonary vascular bed as an aggregate of parallel Starling resistors. **B.** Experimental data on pulmonary resistance, $\Delta P/F$, on ordinate, as a function of right pulmonary arterial pressure in a perfused right lung of the dog. Compare the effect of left atrial pressure (LA) on the relationship curve with that simulated by Permutt's model in Figure 51a. $P_{alv} = 5 \text{ mm Hg}$. (From Permutt et al., 1962).

Because of the non-linear behavior of the pulmonary resistance, the pulmonary artery pressure is less sensitive to net blood flow than would be expected with a constant pulmonary vascular resistance. In addition, the relationship between pulmonary flow and pulmonary artery pressure (or pressure gradient) is non-linear. Figure 52 demonstrates the non-linearities in the flow vs. pressure curve for dog lung.

Pulmonary artery pressure is also relatively insensitive to changes in left atrial pressure, up to LA pressures of 7-10 mmHg. (See Figure 53.) This is because as LA pressure increases, pulmonary vascular resistance decreases (recall Figure 50).

Figure 52

Image removed due to copyright considerations. See Chapter 6 in Fung, Y.C. *Biodynamics: Circulation*. New York: Springer-Verlag, 1984.

Experimental data and theoretical curves relating pulmonary flow and resistance to pulmonary pressure gradient. The experimental data are from an isolated dog lung with pulmonary venous pressure fixed at 3 cm H₂O, pleural pressure equal to zero, and three different alveolar pressures: 23, 17, and 7 cm H₂O. The theoretical curves are based on a model of pulmonary alveolar flow developed by Fung (see Fung 1984, ch. 6).

Figure 53
Effect of left atrial pressure on pulmonary arterial pressure.

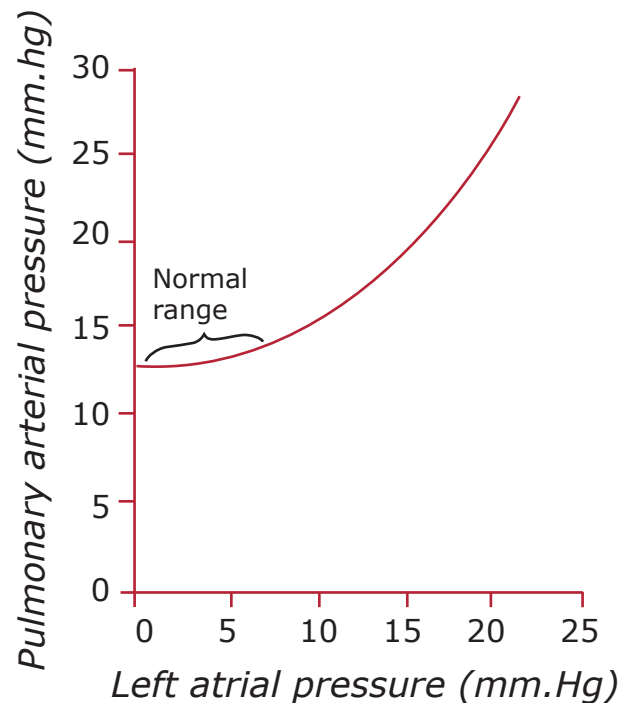


Figure by MIT OCW. After Guyton.

Since the pulmonary artery pressure changes little over wide ranges of flow, we will consider it to be *constant*. Thus, the afterload, P_{PA} , of the right heart is constant, and the RV output is determined only by the properties of the right ventricle, and the RV filling pressure, P_f . In steady state the LV output must exactly match that of the RV. The left atrial pressure adjusts to the proper value such that the stroke volume of the LV equals that of the RV. Therefore, the output of the HLU (referred to as the *cardiac output*), will be

$$C.O. = f(C_D^r P_f - C_S^r P_{PA}) \quad (38)$$

where f is the heart rate in beats per minute, P_f is the filling pressure, P_{PA} is the pulmonary artery pressure, and C_D^r , C_S^r are the diastolic and systolic capacitances of the RV respectively. $C.O.$ is in cc/min.

Notice that the cardiac output is relatively independent of the left ventricular afterload. For example, if the mean aortic pressure were to double from 100 mmHg to 200 mmHg, the left atrial pressure would have to rise by only 3 mmHg (using values for cardiac capacitances given in the table of normal values at the end of this section). This small rise in LA pressure would increase the pulmonary artery pressure even *less* due to a decrease in pulmonary artery resistance. The resultant change in RV output would be only about 5%.

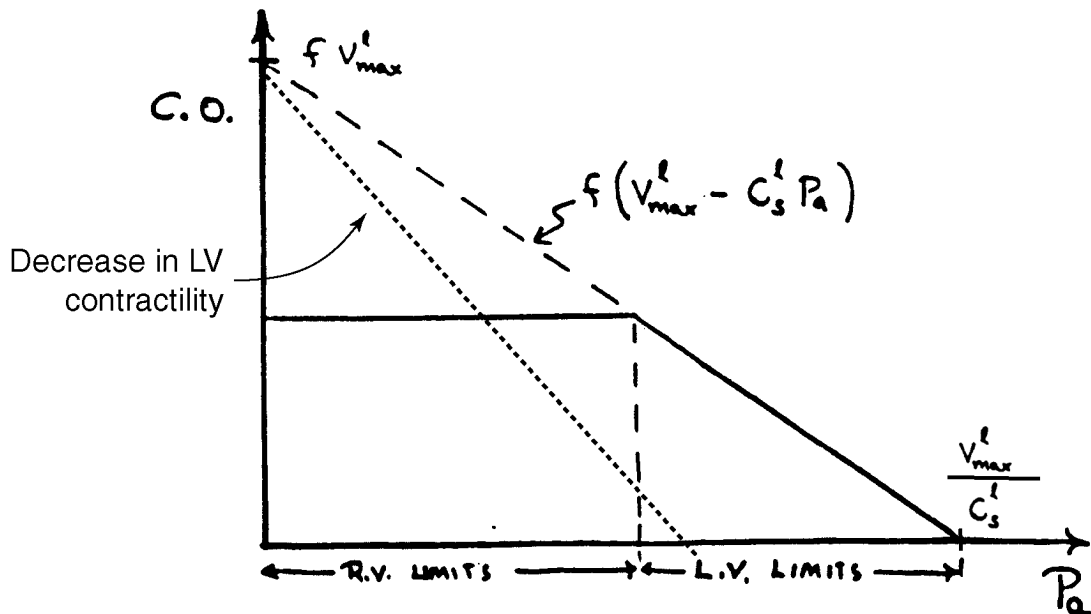
However, there is a limit to the extent to which increasing left atrial pressure will increase left ventricular output. The left ventricle cannot be filled beyond some maximum volume, V_{max} . This limiting volume may be set by the mechanical properties of the ventricular myocardium/pericardium, *but in practice the maximal LV filling pressure is established when the LA pressure reaches the “pulmonary edema” threshold*. At pressures higher than about 30 mmHg, the hydrostatic pressure forcing fluid out of pulmonary capillaries exceeds the oncotic pressure keeping fluid within the vasculature. Water then passes out of the capillaries into the interstitial space, and actually into the alveoli of the lung, leading to the condition known as pulmonary edema. When this condition occurs, gas exchange in the lung becomes impaired, the blood becomes hypoxic, and ventricular function deteriorates still more, which leads to still higher LA pressures and more pulmonary edema. This vicious circle is incompatible with survival unless promptly treated.

When the LV diastolic volume reaches the maximum, then stroke volume cannot exceed

$$SV_{max} = V_{max}^l - C_S^l P_a \quad (39)$$

A plot of cardiac output as a function of systemic arterial pressure, P_a , is of the following form:

Figure 54



At low and normal systemic arterial pressures, the RV determines cardiac output independent of P_a . When the C.O. reaches $f(V_{\max}^l - C_s^l P_a)$, however, the LV begins to limit cardiac output because of its filling limitation. The LA pressure rises, causing concomitant rises in PA pressure, which limits RV output to that set by the left ventricle. Notice that as the LV contractility decreases (increasing C_s) the limiting cardiac output drops. *Thus, the LV will limit cardiac output either at extremely high afterloads, or when LV contractility falls.*

The equations which characterize the heart-lung-unit are shown below.

I. Range I: Cardiac Output determined by RV Function

$$C.O. = f(C_D^r P_f - C_S^r P_{PA}^0) \quad (40)$$

$$\text{when } P_f < \frac{V_{\max}^r}{C_D^r},$$

$$\text{and } P_a < \frac{1}{C_S^l} \left(V_{\max}^l - \frac{C.O.}{f} \right)$$

$$\text{or } P_a < \frac{1}{C_S^l} (V_{\max}^l - C_D^r P_f + C_S^r P_{PA}^0)$$

II. Range II: RV Saturates

$$\begin{aligned} \text{C.O.} &= f(V_{\max} - C_S^r P_{PA}^0) \\ \text{when } P_f &\geq \frac{V_{\max}^r}{C_D^r}, \\ \text{and } P_a &< \frac{1}{C_S^l} (V_{\max}^l - V_{\max}^r + C_S^r P_{PA}^0) \end{aligned} \quad (41)$$

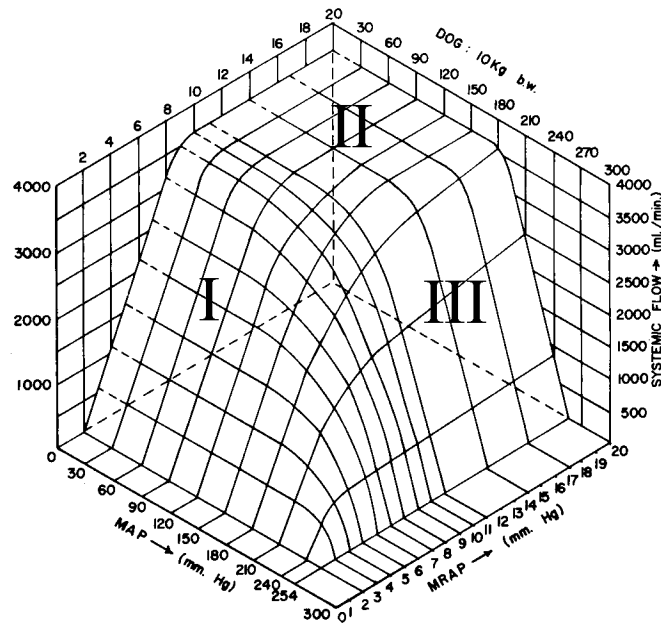
III. Range III: LV Limits C.O. (LV failure)

$$\begin{aligned} \text{C.O.} &= f(V_{\max}^l - C_S^l P_a) \\ \text{when } P_a &> \frac{1}{C_S^l} \left(V_{\max}^l - \frac{\text{C.O.}}{f} \right) \end{aligned} \quad (42)$$

In range I the C.O. depends only on P_f , assuming P_{PA} is essentially constant. In range II the RV diastolic filling is maximum, hence the C.O. saturates (assuming P_{PA} is constant). In range III the C.O. is limited by the left ventricle. **Normally the cardiovascular system operates in range I.**

The equations above may be represented as a three-dimensional plot of C.O. as a function of P_f and P_a . An experimental plot of this sort is shown in Figure 55. The data is from open-chested dogs. The three operating ranges have been indicated on the curves, and show that experimental data seem to fit our simple model reasonably well. Note that for the experimental data, cardiac output was independent of mean aortic pressure up to about 150 mmHg.

Figure 55
Cardiac output as a function of filling pressure and afterload (dog data)
 [Data from Herndon & Sagawa, 1969; figure from Guyton, Jones, and Coleman, 1973.]



2. Effect of Intrathoracic Pressure

Up to now we have treated the heart as it would behave in an open-chested animal. In the intact organism, mean intrathoracic pressure is about 6 mmHg less than atmospheric pressure. The heart senses only transmural pressures. For the same intracardiac pressure relative to atmospheric pressure, the effective transmural pressure is 6 mmHg greater in the closed-chested animal than in the open-chested animal. This effect is particularly pronounced with respect to diastolic filling pressures since these pressures are normally only a few mm of Hg to start off with. Figure 56 explicitly includes the transthoracic pressure into the variable capacitor model.

Figure 56
Electric Circuit Incorporation of Transthoracic Pressure into Variable Capacitor Model.

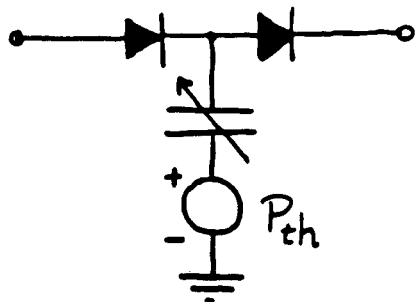


Figure 57 shows three cardiac output curves (at constant afterload) at different transthoracic pressures for humans. In particular, we note that for the normal closed-chest situation there is a substantial cardiac output of approximately 5 L/min at zero right atrial pressure (relative to atmospheric pressure). This is the normal operating point in the closed-chest subject.

Figure 57
Effect on the cardiac output curve of negative pressure breathing, positive pressure breathing, and opening the chest to atmospheric pressure.

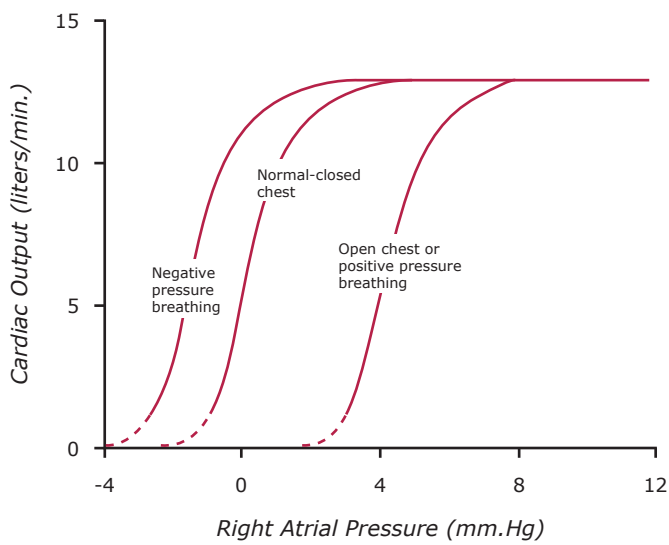


Figure by MIT OCW. After Guyton (1973), Fig. 9-7.

Dr. Arthur Guyton has obtained considerable data on the behavior of cardiac output curves, and students are urged to read his text, "Circulatory Physiology: Cardiac Output and its Regulation": Section II (Guyton 1973.) Some examples of cardiac output curves and their behavior as a function of various interventions are shown below, excerpted from Guyton's book.

Autonomic nervous activity changes cardiac function via rate and contractility mechanisms. This is illustrated in Figure 58. The effect of heart rate alone is shown in Figure 59. Note that at excessively high heart rate cardiac output drops because of insufficient cardiac filling time.

Figure 58
Effects on the cardiac output curve of different degrees of sympathetic and parasympathetic stimulation.

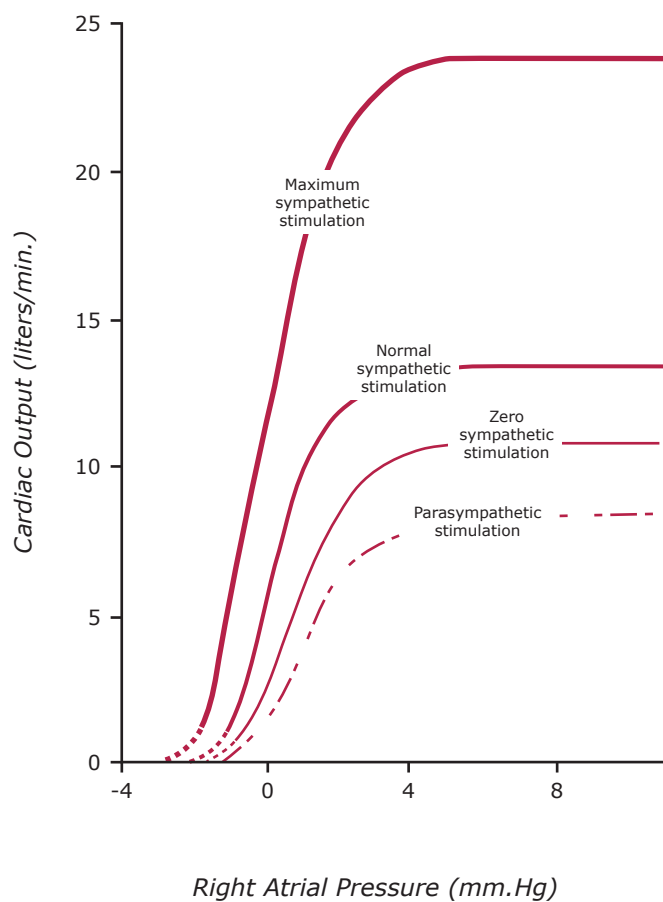


Figure by MIT OCW. After Guyton (1973), Fig. 9-4.

Figure 59
Effect on the cardiac output curve of different heart rates, showing that when the heart is driven electrically, the output becomes optimal at about 125 beats per minute.

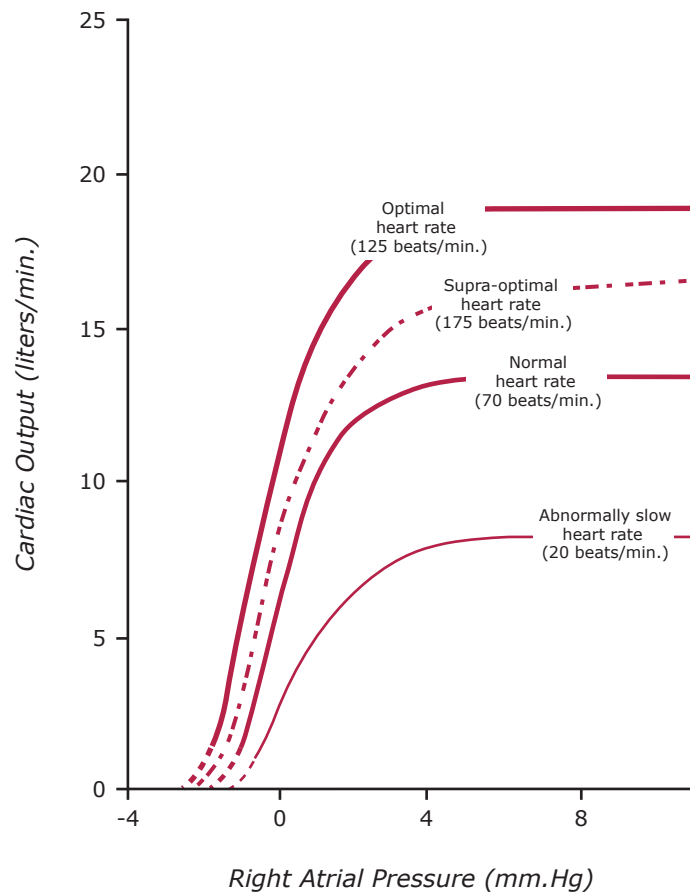


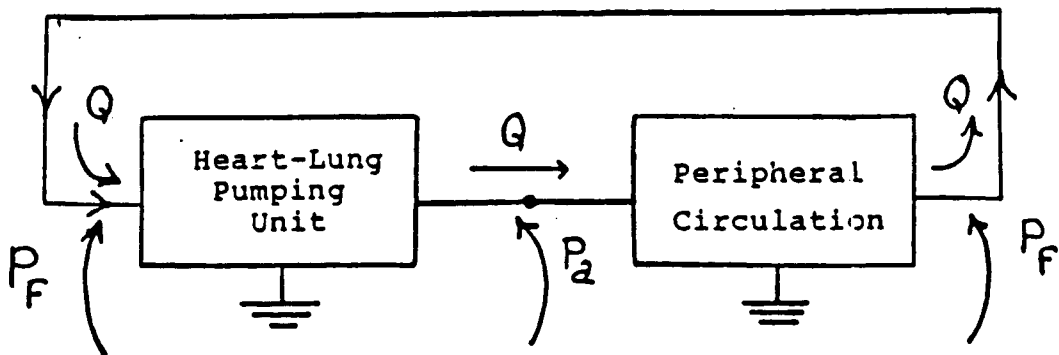
Figure by MIT OCW. After Guyton (1973), Fig. 9-5.

III. MODELLING THE INTACT CARDIOVASCULAR SYSTEM

A. Introduction

We have now developed models for the heart-lung pumping unit and for the peripheral circulation. These models both relate blood flow, Q , to the filling pressure of the right heart, P_f . The two models may be combined as shown in Figure 60.

Figure 60



Since the Q_s and P_{fs} are identical, we may now solve for the steady-state “operating point” of the entire system. Either analytical or graphical techniques may be used. In our analysis we will consider *mean* pressures, flows, and volumes.

B. Normal Functioning of the Cardiovascular System

The equation describing the heart-lung unit in Range I was given in equation 40 above, and is reproduced here. Note that we have explicitly included the effect of intrathoracic pressure, P_{th} .

$$Q = C.O. = f \left[C_D^r (P_f - P_{th}) - C_S^r (P_{PA} - P_{th}) \right] \quad (43)$$

when $P_f - P_{th} < \frac{V_{max}^r}{C_D^r}$,

and $P_a < \frac{(V_{max}^l - S.V.)}{C_S^l}$

The equation governing the peripheral circulation was equation 23 above.

Equations 23 and 43 may be combined to yield an expression for cardiac output.

$$C.O. = \frac{P_{ms} - P_{th} - P_{PA}^0 \frac{C_s^r}{C_D^r}}{R_v + R_a \frac{C_a}{C_a + C_v} + \frac{1}{fC_D^r}} \quad (44)$$

It is useful to put in numerical figures to estimate the importance of the various terms. Using the table of normal values in Table 6 (at the end of the chapter), we find:

$$\begin{aligned} C.O. (\text{cc / sec.}) &= \frac{8 + 5 - 1.5}{.06 + .02 + .05} \\ &= 84.6 \text{ cc / sec.} \\ &= 5.07 \text{ L / min.} \end{aligned} \quad (45)$$

Based on equation 45 we may examine the principal determinants of the cardiac output in the normal physiologic range.

1. *Heart Rate.* Cardiac output increases asymptotically with heart rate in this model. Notice that if the heart rate goes to zero, the last term in the denominator goes to infinity and C.O. goes to zero. As heart rate gets very large, this term gets vanishingly small and cardiac output reaches an asymptotic value of 8.6 L/min. in our case. (Note that our model does not take account of the drop in C.O. as filling time decreases.)
2. *Mean Systemic Pressure, P_{ms}.* This term is the largest in the numerator, and is a major determinant of cardiac output. Since P_{ms} is the ratio of distending blood volume to total systemic capacitance, a change in either of these factors will alter P_{ms} and hence cardiac output. Increasing blood volume, decreasing venous capacitance, or decreasing venous zero-pressure filling volume will lead to increased C.O.
3. *Intrathoracic Pressure, P_{th}.* This term is an important one, and makes a major contribution to cardiac output by virtue of its action on cardiac filling. (You should know what happens in a *Valsalva maneuver*.)

4. *Venous Capacitance, C_v .* This term appears explicitly in the second term in the denominator (a small term) and implicitly in the definition of P_{ms} in the numerator. As C_v increases, C.O. decreases.
5. *Right Ventricular Diastolic Capacitance, C_D^r .* Increasing C_D^r will increase the numerator and decrease the denominator, hence increasing cardiac output (in a saturating manner). (Generally this variable will not change, however.)
6. *Arterial Resistance.* Varying R_a has only a small effect on C.O. R_a enters only the small second term in the denominator. What effect does R_a have on P_a ?
7. *Arterial Capacitance, C_a .* Since $C_a \ll C_v$, C_a essentially enters the second term of the denominator in the form $R_a C_a$. Varying C_a will have a rather small effect on C.O.
8. *Venous Resistance, R_v .* Increasing R_v dramatically increases the first term of the denominator, and drops C.O.
9. *Inotropy of the Ventricle.* Under normal conditions the cardiac output is weakly dependent on C_s^r and completely independent of C_s^l . This reflects the fact that the contractility of the ventricles is not the major factor limiting cardiac output; rather it is the diastolic filling of the RV.

C. Cardiac Output Under Abnormal Conditions

We now consider the abnormal operating ranges of the heart-lung pump.

1. Range II

Range II is defined by maximum filling of the right ventricle

$$P_f - P_{th} \geq \frac{V_{max}^r}{C_D^r},$$

and $P_a < \frac{V_{max}^l - S.V.}{C_S^l}$

In this range the left ventricular output is not constrained, but the R.V. has *fixed output* which determines overall C.O.

$$C.O. = f[V_{max}^r - C_S^r(P_{PA} - P_{th})] \quad (46)$$

2. Range III

The system is in range III when the left ventricle is the limiting chamber in determining cardiac output. From equation 36 the maximum stroke volume obtainable from the L.V. is given by:

$$S.V.|_{max} = V_{max}^l - C_S^l P_a$$

Thus, when

$$P_a > \frac{1}{C_S^l} (V_{max}^l - S.V.) \quad (47)$$

The L.V limits cardiac output to:

$$C.O. = f(V_{max}^l - C_S^l P_{PA}) \quad (48)$$

But

$$P_a = P_v + (R_a + R_v)(C.O.)$$

If we simplify this relationship by ignoring P_v and assuming $R_v \ll R_a$ we obtain

$$P_a \cong (C.O.)(R_a) \quad (49)$$

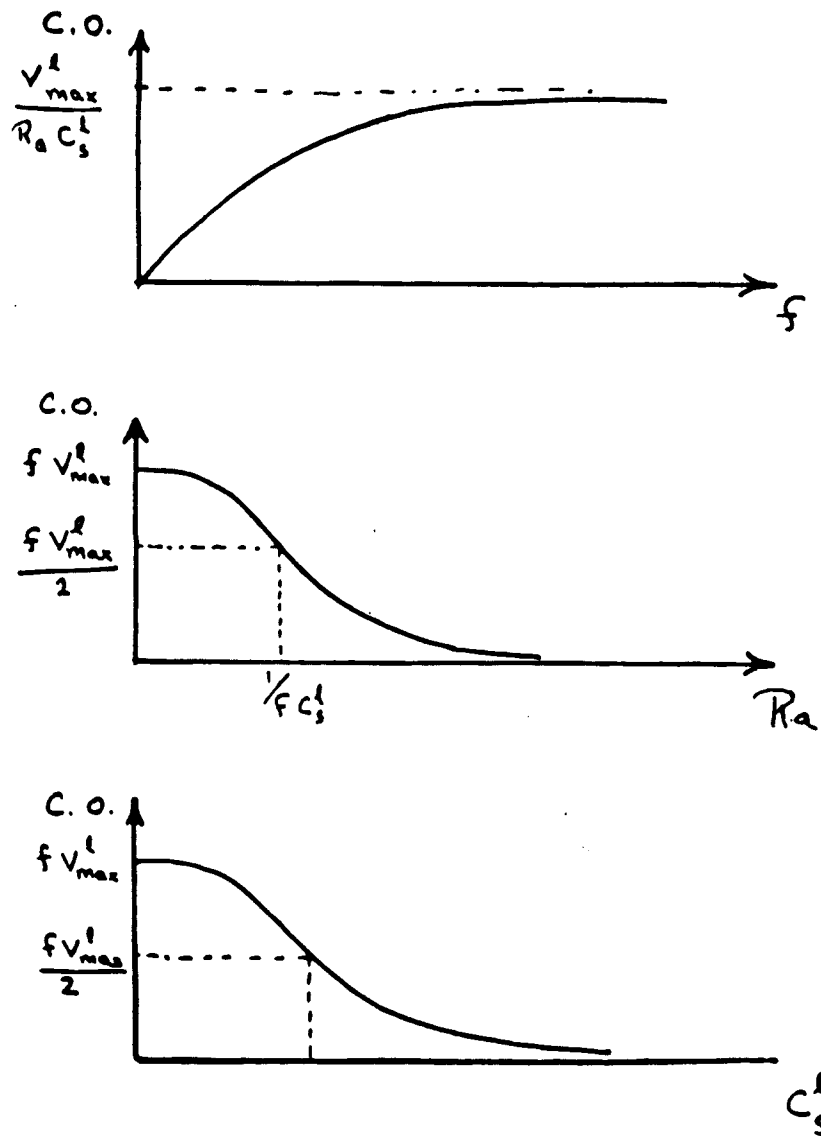
Substituting (49) into (48) we obtain

$$C.O. = \frac{fV_{max}^l}{\left(1 + fC_S^l R_a\right)} \quad (50)$$

Thus, under conditions of LV-limited cardiac output, the cardiac output is a function of LV contractility, C_S^L ; peripheral arterial resistance R_a ; and heart rate, f . Note that C.O. increases asymptotically with increasing heart rate; decreases with increasing C_S or R_a . (See Figure 61.) Inequality (47) is satisfied at either extremely high systemic pressures, or more commonly in *left ventricular failure* when C_S becomes larger than normal.

It is under these conditions that “afterload reduction” (decrease in R_a) is effective in increasing cardiac output.

Figure 61
Cardiac Output when limited by L.V. (Range III)



D. Graphical Solution

1. Operating Point Analysis

The graphical solution for the steady-state operating point of the intact circulation makes use of the “venous return” and “cardiac output” curves, and was introduced by Dr. Arthur Guyton. Figure 62 shows normal cardiac output and venous return curves. The point of intersection is the operating point. Note that the steady state operating point is at a C.O. of 5 liters/min. and a right atrial pressure of 0 mmHg (referenced to atmosphere in a closed-chest individual).

Figure 62

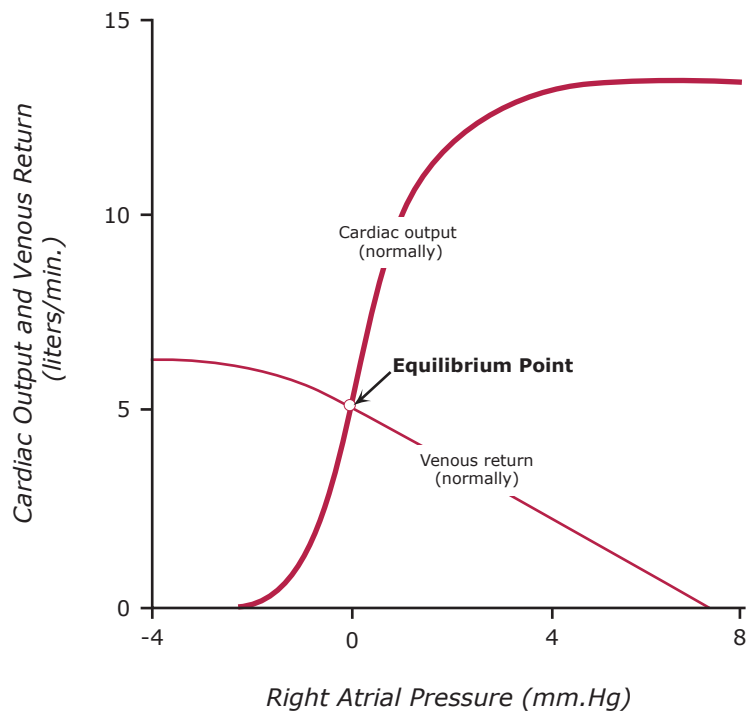


Figure by MIT OCW. After Guyton (1973), Fig. 14-1.

In the following section, we will illustrate the use of Guyton’s graphical technique to analyze several specific physiological states.

2. Sympathetic Stimulation

- Sympathetic stimulation has rather little effect on *resistance to venous return*, R_v .

- Sympathetic stimulation causes constriction of veins with a decrease in zero-pressure filling volume, and increased mean systemic filling pressure—hence, moves venous return curves up and to the right.
- Sympathetic stimulation increases peripheral resistance, and the slope of the venous return curve decreases. This is a *small* effect compared to the change in P_{ms} , however.
- Sympathetic stimulation changes the cardiac output curves by shifting to the left and increasing the slope. This is due to increases in both contractility and heart rate.

Figure 63 illustrates an analysis for the combined effects of sympathetic stimulation on both cardiac and peripheral factors. The normal operating point is at A, while with increased sympathetic tone, the operating point moves from A to C, and then to D. Notice that despite the increase in cardiac output, RA pressure drops. These curves do not show arterial blood pressure. What would you expect to happen to blood pressure under intense sympathetic stimulation?

Figure 63

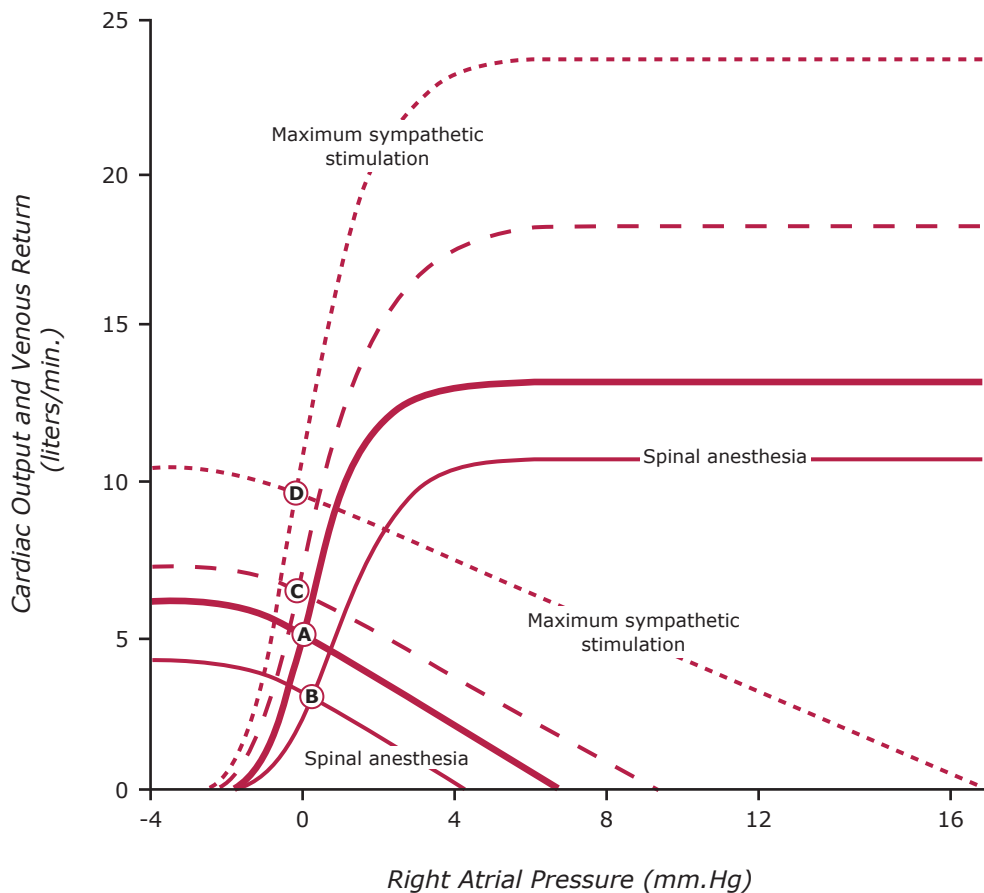


Figure by MIT OCW. After Guyton (1973), Fig. 18-4.

3. Tissue Oxygen Need

Hypoxia leads to vasodilation. Thus, if a vascular bed is perfused with blood with an O₂ saturation of only 30%, a prompt vasodilation is observed. Hypoxia will shift the C.O. curve downward and to the right—with severe hypoxia seriously damaging the heart's ability to pump. Figure 64 illustrates the impact of two degrees of hypoxia on cardiac output.

Figure 64

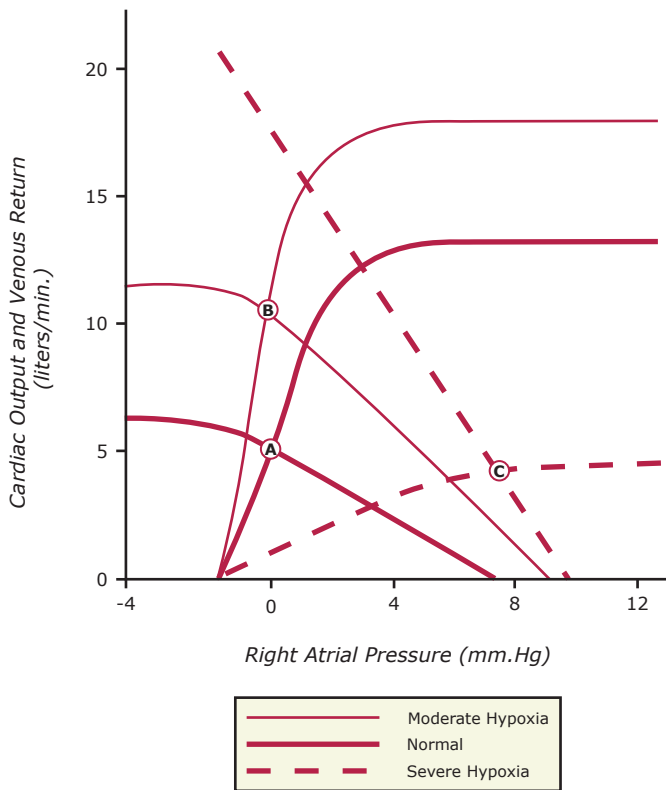


Figure by MIT OCW. After Guyton (1973), Fig. 19-13.

4. Muscular Exercise

The most stressful condition to the normal circulatory system is vigorous exercise. Well-trained athletes may increase their cardiac outputs by up to 6 or 7 times normal. Exercise can affect cardiac output in several ways:

1. Tensing of muscles, especially those in the abdomen and legs, can increase mean systemic pressure, thus increasing venous return.
2. Autonomic stimulation will increase mean systemic filling pressure and also increase cardiac contractility and rate.
3. Increase in muscle metabolism causes local vasodilatation which decreases the resistance to venous return. The time sequence of the effects is shown in Figure 65.

Figure 65

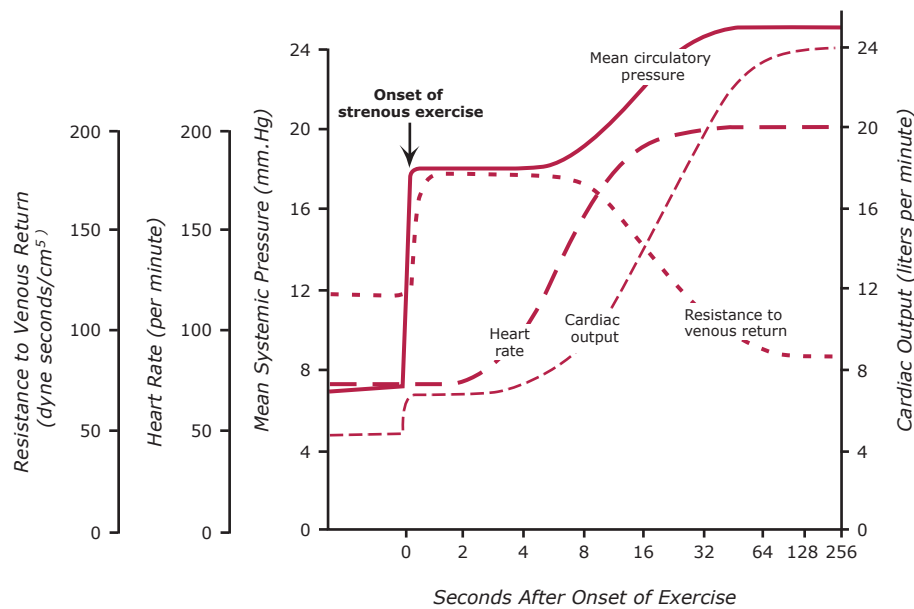


Figure by MIT OCW. After Guyton (1973), Fig. 25-2.

The graphic analysis shown in Figure 66 illustrates the net effect on cardiac output. The normal operating point is at A. At the onset of *moderate* exercise, the tensing of muscles leads to an immediate increase in MSP from 7 mmHg to 10 mmHg, and the operating point moves to B. Note that the resistance to venous return on this venous return curve has *increased* slightly due to muscle clamping. The CO increases from 5 L/min to about 6 L/min. During the next 15 to 20 seconds sympathetic stimulation becomes significant, causing both cardiac and peripheral effects. Both CO and venous return curves shift appropriately, and the next operating point is at C with a cardiac output of 8 L/min at an RA pressure of 0. Finally, metabolic dilatation of the muscular vascular bed occurs, resulting in decreased resistance to venous return. The new equilibrium point at D shows a CO of 13 L/min at an RA pressure close to zero.

Figure 66
Graphical analysis of the changes in cardiac output and right atrial pressure at various time intervals following the onset of moderate exercise.

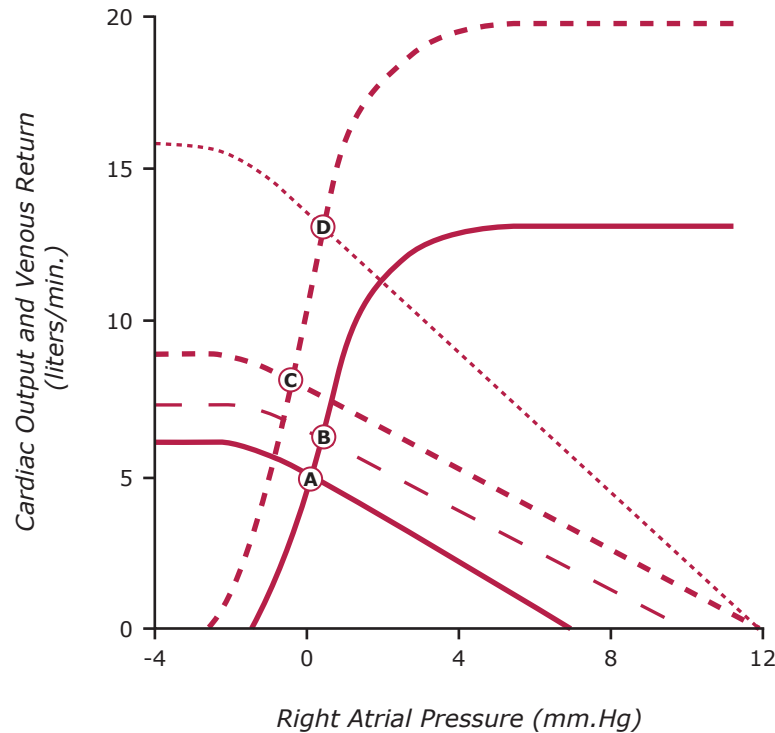


Figure by MIT OCW. After Guyton (1973), Fig. 25-3.

Table 6
Glossary of Symbols and Nominal Value for Model Parameters

Symbol	Definition	Normal Value
ΔV	Stroke Volume	96 cc
$f = 1/T$	Heart Rate	60/min.=1/sec.
$T = T_s + T_d$	Duration of Heart Cycle	1 sec.
T_s	Duration of Systole	.3 sec.
T_d	Duration of Diastole	.7 sec.
C_D^r	Diastolic Capacitance of RV	20/ml/mmHg
C_D^l	Diastolic Capacitance of LV	10 ml/mmHg
C_S^r	Minimum Systolic Capacitance RV	2 ml/mmHg
C_S^l	Minimum Systolic Capacitance LV	.4 ml/mmHg
V_{\max}^r, V_{\max}^l	'Maximum' Volumes, RV, LV	200 cc
$V_T = V + V_0$	Total volume of blood in peripheral vasculature	4000 ml
V_0	Volume needed to fill peripheral vasculature without increasing pressure	3200 ml
C_a	Arterial Capacitance	2 ml/mmHg
C_v	Venous Capacitance	100 ml/mmHg
R_a	Arterial Resistance	1 mlHg/(ml/sec)
R_v	Resistance to Venous Return	.05 mmHg/(ml/sec)
P_{th}	Mean Intrathoracic Pressure	-5 mmHg
P_A^0	Pulmonary Artery Pressure (End-Systolic) referenced to mean intrathoracic pressure	15 mmHg
P_{ms}	Mean Systemic Filling Pressure (see text)	7.8 mmHg
P_v	Peripheral Venous Pressure	6.1 mmHg

Selected References

- Caro, L.G., et al. 1978. *The Mechanics of the Circulation*, Oxford University Press. This book considers a number of issues concerning cardiovascular fluid mechanics. It is written in a style which should be understandable to most engineering students, and does not assume a strong background in fluid mechanics.
- Frank, O. 1888. *Zeitschrift fur biologie* 37:483.
- Fung, Y.C. 1984. *Biodynamics: Circulation*. Springer-Verlag. This book presents a rather detailed discussion of the fluid mechanics of the circulation, considering mechanics of the heart; flow in arteries, veins, microcirculation, and lung.
- Guyton, A.C. 1973. *Circulatory Physiology: Cardiac Output and its Regulation*, 2nd ed. Saunders. This volume develops the cardiac output/venous return curve approach and gives many interesting examples. Although old, it is a classic will worth reading.
- Holt, J.P. 1969. Flow through collapsible tubes and through in situ veins. *Trans. Biomed. Eng.* BME-16: 274-283.
- Katz, A.M. 2000. *Physiology of the Heart*, 3rd. ed., Lippincott Williams & Wilkins. A good overview of cardiac physiology with particular strength in electrophysiology and excitation-contraction coupling.
- Mukkamala, R. 2000. A Forward Model-Based Analysis of Cardiovascular System Identification Methods. Ph.D. thesis, Massachusetts Institute of Technology.
- Opie, L.H. 1998. *The Heart: Physiology from Cell to Circulation*. Lippincott-Raven Publishers.
- Sagawa, K. 1973. Comparative models of overall circulatory mechanics. *Advances in Biomedical Engineering*, Vol. 3, ed. JHU Brown and J. Dickson. Academic Press, pp. 1-95. This review article considers a wide range of models which have been used to describe the heart and circulation. It will provide a good introduction to the early literature.
- Sunagawa, K. and Sagawa, K. 1982. Models of ventricular contraction based on time-varying elastance. *CRC Critical Reviews in Biomedical Engineering*, vol. 7, issue 3. This complete review summarizes the extensive work of Professor Sagawa on modeling the ventricle as a time-varying elastance. It will be of great interest to students who wish more detail, and experimental verification of this modeling approach.

Cardiovascular Mechanics — Index

- Afterload.....31, 34-37, 40, 43, 44, 48, 50, 51, 53, 56, 59, 63, 64, 67
Afterload reduction75
Calcium.....27, 28, 30, 39
Capacitance.....3, 6, 7, 12-15, 23, 24, 41-43, 45, 53, 63, 72, 73, 82
 arterial.....11, 23-25, 73, 82
 diastolic.....41, 73, 82
 end-systolic.....49, 56
 vascular5, 9, 15
 ventricular42
Cardiac output.....4, 25, 33, 37, 43, 63-69, 72-81
Cardiac output curves.....67-69, 76, 78
Collapsible tubing.....16
Compliance.....41, 54
Contractility37-40, 51, 53, 54, 57, 64, 68, 73, 75, 78, 79
Cross-bridges27, 29
Diastole.....25, 31, 34, 37, 40-42, 46, 82
Diastolic Pressure.....25, 31, 33, 34, 37, 39, 41, 49, 54
Distending volume15
Ejection Phase.....45
Elastance54
Electrical/Mechanical Analogies.....12
End-diastolic pressure.....33, 34, 37, 54
Graphical Solution76
Heart-lung pumping unit.....59, 60, 64, 71, 73
Hooke's Law9, 11
Hypoxia.....78, 79
Intrathoracic Pressure66, 71, 72, 82
Isometric contraction.....31, 51
Isovolumetric contraction.....34, 37, 52
Isovolumic contraction45
Isovolumic relaxation45
Law of the Heart33, 37
Length-tension relationship.....27, 29, 30
Mean pressure4, 25, 71

Mean systemic pressure, P_{ms}	15, 21, 22, 72, 77, 79
Model	3, 7, 8, 13, 22, 23, 25, 27, 31, 40, 44, 49, 51, 53, 59-62, 65-67, 71, 72, 82
Model of the Heart.....	40
Muscular Exercise	79
Operating point.....	37, 67, 71, 76-78, 80
Peripheral Circulation	3, 13, 14, 20, 22, 23, 27, 71, 72
Peripheral resistance units.....	4
Poiseuille flow	3
Poiseuille's law.....	5, 86
Positive inotropic agent.....	39
Preload.....	31, 34-38, 40, 43, 44, 48, 50-53, 59
Pressure-volume loop	34-36, 40, 46, 52-54, 57, 58
Pulmonary artery pressure.....	60, 61, 63, 82
Pulmonary edema	63
Pulmonary resistance.....	61
Pulmonary vascular bed.....	3, 59-61
Pulse Pressure	25
Right atrial filling pressure.....	13, 59
Sarcomeres	27, 28
Sarcoplasmic reticulum.....	27, 28, 39
Starling resistors.....	16, 60, 61
Starling's Law	33
Strain	8, 9, 74, 86
Stroke work	33, 37
Sympathetic Stimulation	68, 77, 78, 80
Systemic vascular bed.....	3
Systolic pressure	24, 31, 34, 38, 52
Vascular Resistance	3, 4, 23, 59, 60, 61
Venous return	3, 16, 18-22, 76, 77, 79, 80, 82
Venous return curve	18-22, 77, 80